# Thermodynamics and vapourization of Cs-, Sr-, Ba-containing oxide systems valid for nuclear safety problems †

**Valentina L.Stolyarova,**[a, b] **Andrey L. Shilov,**[a, b] **Tamara V. Sokolova,**[b] **Masaki Kurata,**[c] **Davide Costa** [d]

[a] *Saint Petersburg State University,*
*Universitetskaya nab. 7 – 9, 199034 Saint Petersburg, Russian Federation*
[b] *I.V.Grebenshchikov Institute of Silicate Chemistry, Russian Academy of Sciences,*
*Makarov nab. 2, 199034 Saint Petersburg, Russian Federation*
[c] *Collaborative Laboratories for Advanced Decommissioning Science, Japan Atomic Energy Agency,*
*Fukushima, 979-1151 Japan*
[d] *Division of Nuclear Science, Nuclear Energy Agency OECD,*
*Quai Alphonse Le Gallo 46, Boulogne-Billancourt, 92100 France*

The review provides a systematic analysis of the studies carried out mainly in the last decade in which the thermodynamic properties and vapourization of the systems containing cesium, strontium, and barium were studied by high-temperature mass spectrometry. Such systems are of particular interest for considering the problems of environmental safety in the nuclear power industry. Particular attention is paid to the issues of reliable identification of the content of the gaseous phase over oxide systems, which are important in various high-temperature technologies, including the disposal of radioactive waste, reprocessing of nuclear fuel, as well as ensuring the safe operation of nuclear power plants. A discussion and comparison of thermodynamic data found in the literature for the systems under consideration in a wide temperature range were also carried out featuring the main advantages of the Knudsen mass spectrometric effusion method.
The bibliography includes 117 references.

## Contents

† Dedicated to the 300th Anniversary of Saint Petersburg State University.

2 of 22

V.L.Stolyarova, A.L.Shilov, T.V.Sokolova, M.Kurata, D.Costa
*Russ. Chem. Rev.*, 2023, **92** (5) RCR5059

# 1. Introduction

The results of high-temperature mass spectrometric studies of the vapourization processes in oxide systems containing cesium, strontium and barium oxides published during the last 20 years are quoted and analyzed in the present review. Investigations of the vapour composition and partial pressures of its components over oxide systems as well as evaluation of the thermodynamic properties of the systems on the basis of these data have been carried out for more than a hundred years already with the use of various direct and indirect methods, such as the transpiration method, the method of boiling points, thermogravimetry and *etc*. But of course, the most informative and all-embracing is the high-temperature Knudsen effusion mass spectrometric method (KEMS), which principally enables the measurement of the partial pressures of all essential components of the vapour over samples in a wide temperature range up to 3000 K and in some particular cases allows determination of thermodynamic activities of components directly from the measured values of the ion currents. The benefits of this method and its fundamental role in the present-day research have been broadly discussed in the literature.[1-4] It was demonstrated that the thermodynamic data obtained using high-temperature mass spectrometry (HTMS) or KEMS as its particular modification make possible predicting the high temperature behaviour of the systems under study. This information is necessary for development of new methods of synthesis of materials for high-temperature applications.[5] Examination of the data referring to the systems based on $Cs_2O$, SrO, and BaO reported in recent years is important for both fundamental thermodynamic studies and handling different ecological issues especially the ones concerning the nuclear safety problems.

The choice of the systems containing cesium, strontium, and barium is reasonable since these are the elements forming during fission of radioactive fuel in nuclear power plants (NPPs) and as a result of heavy accidents, which can release into the environment and present serious ecological hazards. It should be noted that interest in these systems has existed for a long time. For example, pioneering studies by the HTMS method of the systems containing cesium compounds were carried out by L.N.Gorokhov with co-authors[6,7] in the 70s and successfully continued in their further work.

The data on the vapourization behaviour and thermodynamic properties of Cs-, Sr- and Ba-containing systems

**V.L.Stolyarova**. Academician of RAS, Professor of the Saint Petersburg State University, Head of the Laboratory at the Institute of Silicate Chemistry of RAS, Doctor of Chemistry.
E-mail: v.stolyarova@spbu.ru
**A.L.Shilov**. Leading Researcher at the Institute of Silicate Chemistry of RAS, PhD in Chemistry.
E-mail: naskalinen@mail.ru
**T.V.Sokolova**. Leading Researcher, PhD in Technical Sciences.
E-mail: tv_sokolova@mail.ru
*Research interests of the authors*: physical and inorganic chemistry, materials science, high temperature mass spectrometry, thermo-dynamics, modelling, oxide systems and materials.
**M.Kurata**. Head of the Division, Doctor of Chemistry.
E-mail: kurata.masaki@jaea.go.jp
**D.Costa**. Project Leader, Doctor of Chemistry.
E-mail: Davide.COSTA@oecd-nea.org
*Research interests of the authors*: physical and inorganic chemistry, materials science, thermodynamics, modelling, oxide systems and materials, nuclear safety problems.

obtained using high temperature mass spectrometric method were discussed and summarized in the mono-graphs[8,9] and recently in Ref. 10. Thus, reviews of all publications on this topic which appeared before 2004 related to the corresponding binary and multicomponent systems containing $B_2O_3$, $Al_2O_3$, $CO_2$, $SiO_2$, $N_2O_5$, $P_2O_5$, $SO_3$, $H_2O$, $Cr_2O_3$, $MoO_3$, $WO_3$, $Re_2O_7$, $TeO_2$, $Sb_2O_3$, $As_2O_5$, $V_2O_5$, $Nb_2O_5$, $Ta_2O_5$ and $UO_2$ may be found in Refs 8, 9. It should be mentioned that in the present review the recent data published during mainly the last ten years will be considered.

Fierce ecological problems that mankind have been facing and may still encounter after severe reactor accidents at NPPs stimulate all kinds of research aimed at diminishing the relevant risks. The experts insist that the perils of such catastrophic events are permanently on the agenda.[11,12] They may arise from wear and tear of the facilities, natural disasters, human factor, and the threat of nuclear terrorism.

About 200 NPPs are in operation today around the world and many of them are running already for more than 30 years (commissioning safe operation warranty term). The share of nuclear power in the energy production is relatively high in the USA (roughly 100 reactors), France (roughly 50 reactors), and Russia (roughly 40 reactors). After severe accidents at Chernobyl (April 1986) and Fukushima (March 2011) power plants some of the techno-logically developed countries such as Germany and Italy have switched over to phasing out nuclear power genera-tion. However, this policy is unacceptable for the states whose energy production cannot be based only on the fossil fuel and alternative sources of energy. For example, the share of atomic energy in the total energy production in France was 70% in 2020 year and as a matter of fact this branch of industry ensures national independence of the country in power production. Nuclear power production grows at high rate in China. Twenty power-generating units are projected for construction in Great Britain to make possible switching off of the motor transport to electric vehicles. Until 2011 atomic energy production developed rapidly in Japan providing up to 30% of the country's power supply. After the reactor accident at Fukushima operation of nuclear power plants was suspended for rehabilitation and in the nearest future is going to be restarted. A considerable part of the total power production about 20% in 2020 year is provided by NPPs in Russia.[13] Development of this branch of industry is dictated by the need for diversification of energy sources that must be regarded as a matter of the state security and its stable economic growth. It should be remembered also that if safety regulations are strictly observed, nuclear reactor operation is less polluting to the environment in comparison with fossil fuel power plants with no emission of greenhouse gasses and toxic substances. Summing up and bearing in mind gradual depletion of fossil fuel reserves and limited capacity of renewable sources of energy one may conclude that there is no alternative to atomic energy production.[14,15]

There were about one hundred accidents in the history of nuclear power production. In 1990 the International Atomic Energy Agency (IAEA) introduced the International Nuclear Event Scale (INES) for evaluation of the accidents related to radioactive release into the environment. Two events up to now were assigned the highest 7th level on the INES scale, these were the Chernobyl and Fukushima Daiichi nuclear power plants disasters. Nuclear release lead to pollution of soil and water with radioactive

V.L.Stolyarova, A.L.Shilov, T.V.Sokolova, M.Kurata, D.Costa
*Russ. Chem. Rev.*, 2023, **92** (5) RCR5059

3 of 22



**Figure 1.** Cross-section of the core catchers: (*a*) is with ceramic sacrificial material for the prospective WWER reactor (Russia) and (*b*) is with concrete sacrificial material for the Eu-APR1400 reactor (South Korea).[35]

nuclides and pollution of atmosphere with aerosols and radioactive inert gasses.[16–21]

The safety and efficiency issues in the nuclear industrial applications have always drawn great attention and hence the engineering design and operation of nuclear power plants have always been based on a solid scientific background provided by R&D projects organized and coordinated by the Organization for Economic Co-operation and Development, the International Atomic Energy Agency, the Atomic Energy Society of Japan, the UK Atomic Energy Authority, the United States Department of Energy and other bodies and institutions. A lot of information is accumulated on various aspects of the nuclear power plants performance and possible reactor core accidents including the data on the formation of gaseous radioactive emissions, volatility and thermodynamic properties of components of the substances and construction materials involved in these processes and relevant physicochemical reactions.

In the earlier atomic energy history, the knowledge of volatility of the nuclear materials was necessary mainly for assessment of the impact of nuclear power plants on the environment, of the long-term consequences of the radioactive waste storage, and radioactive emissions release in reactor core failures. After the Chernobyl and Fukushima severe accidents in the list of subjects to be considered were included such points as development of methods and instruments for monitoring the contamination of the polluted sites,[22] detailed study of the processes occurring in the destroyed nuclear reactor core, and the strategy of decommissioning of nuclear power plants after severe accidents. Solution of these problems requires combined efforts and coordinated research programs implemented, for example, in such projects as TCOFF, BSAF-2, Pre-ADES, and SAFEST.[23] The general aim of the research works is to reduce practically to zero the probability of severe accidents in the nuclear reactors of the fourth generation (Gen IV).
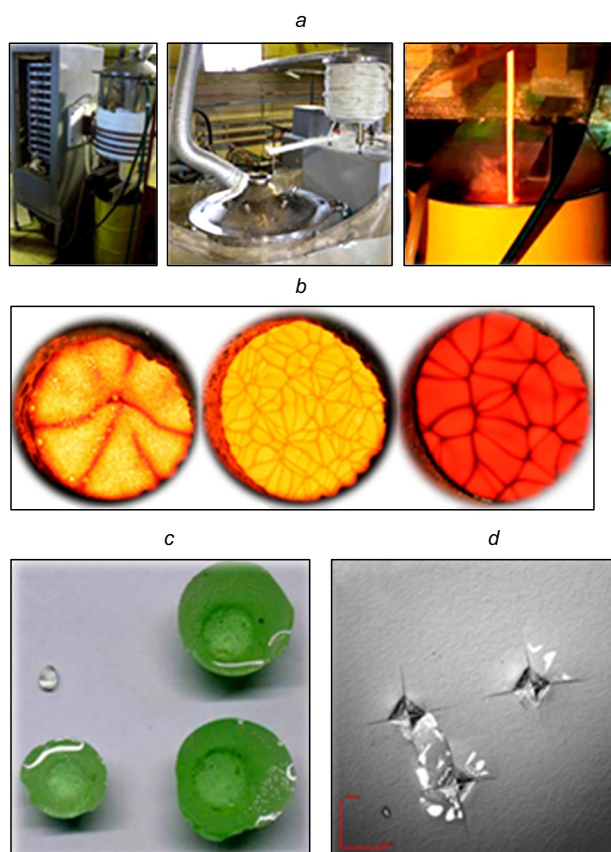
Investigation of volatility of materials components at high temperatures characteristic of the nuclear reactor core remains urgent and indispensable. Current studies, a considerable part of which is based on high-temperature mass spectrometry, are focused on improvement of the reliability of the experimental data and the obtained thermodynamic functions and on the investigation of the oxide systems not yet explored, the most important of which in the field of nuclear power production are the systems based on cesium, strontium, and barium oxides.

It should be specially underlined that the high-temperature mass spectrometric method enables simultaneous acquisition of the highly important information on both the vapourization processes and the thermodynamic properties of a substance under study at high temperatures. On the one hand, these mutually complementary data can be used for solving the ecological problem of eliminating the radionuclides release into the atmosphere and on the other hand, they allow to predict phase equilibria in the multicomponent materials actual for various nuclear technologies, for example, at the stages of heavy accidents at nuclear power plants or nuclear waste disposal. Thus, the aggregated data on the vapourization processes and the thermodynamic properties of the $SrO-SiO_2$ system at high temperatures,[24–26] allowed to effectively develop ceramic oxide materials applicable in the facilities for localization of a nuclear reactor core melt.[27–29] Though the development of this type of equipment was initiated only in 1998, the concept of the system of external localization of the melt at the presently running units of nuclear power plants with Water–Water Energetic Reactor (WWER) is now already formulated and this success not only makes possible achieving higher levels of their operational safety, but also extends their lifetime.[30–34] Schematic of the facilities for the core melt localization and sacrificial concretes for the projected NPP with WWER (*a*) and for the Eu-APR1400 reactor, South Korea, (*b*) are shown in Fig. 1 reproduced from Ref. 35.

Preventing the evapouration into the environment of the radioactive Cs-, Sr-, and Ba-nuclides during high-level and medium-level radioactive waste disposal into the phosphate and borosilicate glass crystalline matrixes nowadays is also impossible without the reliable information on the vapourization processes and the thermodynamic properties of the oxide systems allowing to analyze correctly the relevant high-temperature physicochemical processes.[33–36] Single-stage technology of high-level radioactive waste vitrification in phosphate matrixes designed in the Alexandrov Research Institute of Technology is shown in Fig. 2.[35] New developments in glassy nuclear waste forms were considered in detail in the monograph by Ojovan and Lee.[36] General problems and advancement dealing with the incorporation of nuclear waste of various compositions mainly in borosilicate glasses were also shown and overviewed in this book including preferable installations used for these purposes as shown on Figs 3 and 4.[36] Figure 3 illustrates a cold crucible melter with agitating unit for immobilization of waste in a glass composite material (*a*) and also a photograph of melt pouring from the cold crucible melter (*b*).[36]

In addition to these examples of the long-term high-temperature processes taking place in nuclear technologies mentioned above the recent modern approach of incorporation of nuclear waste should also be mentioned, that is thermal treatment of nuclear waste of the high-level activity together with the oxide charge during re-propagating high

4 of 22

V.L.Stolyarova, A.L.Shilov, T.V.Sokolova, M.Kurata, D.Costa
*Russ. Chem. Rev.*, 2023, **92** (5) RCR5059

**Figure 2.** Single-stage technology of radioactive waste vitrification realized in the Alexandrov Research Institute of Technology: (*a*) are the crucible, pulp feeding system, and pouring of glass melt into a container; (*b*) is surface of the glass melt (convection pattern on the surface); (*c*) are samples of vitrified radioactive waste; (*d*) is examination of microhardness of the samples of vitrified radioactive waste.[35]

temperature synthesis with the initiation of the combustion reaction of the charge components.[37]

Taking into consideration the practical requirement to avoid the presence, for example, of cesium and its compounds in the environment, the special approach to analysis of cesium isotope distribution was developed using thermal ionization mass spectrometry with the purpose to analyze of radioactive contamination in Fukushima prefecture.[38] Recent report should be also mentioned on the experimental setup for the *in situ* work function and cesium flux measurements, suitable for cesium seeded negative hydrogen ion source for fusion applications.[39] The effective approach to the radioactive gaseous cesium collection was suggested recently using ceramic sorbent.[40] Some earlier information available on cesium and strontium compounds vapourization published before 1996 may also be found in Ref. 41.

Obviously, in all examples mentioned above, the additional knowledge on the vapourization processes and thermodynamic properties of the Cs-, Sr-, Ba-containing systems and materials is required to minimize the harmful evapouration to the environment and for the development of various types of materials to prevent this effect based on thermodynamic approach.

Thus, the objective of the present review fully corresponds the set of problems formulated in the Strategy for Scientific and Technological Development of the Russian Federation, which states, in particular, the urgency to boost
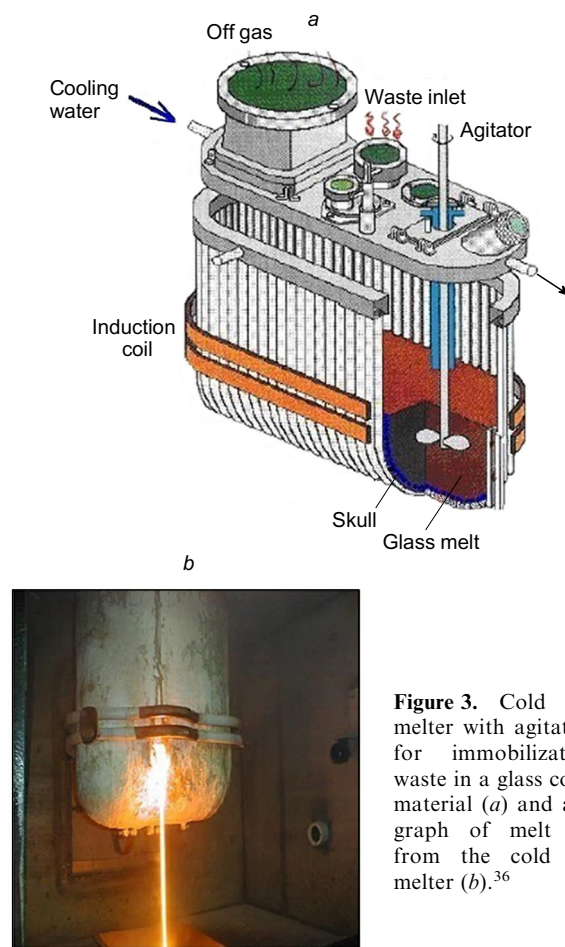


**Figure 3.** Cold crucible melter with agitating unit for immobilization of waste in a glass composite material (*a*) and a photograph of melt pouring from the cold crucible melter (*b*).[36]



**Figure 4.** View of a cold crucible melter with a piece of glass manufactured in it (*a*) and a view of this piece with the protective layer made of glass batch material (skull) which separates the glass melt inside the cold crucible melter from its water-cooled tubes (*b*).[36]

'... a switch to ecologically pure and resource-saving energy production, improvement of efficiency of extraction and deep processing of hydrocarbon raw materials, development of new sources of energy and methods of its transportation and storage.'‡ It should be acknowledged also that the study and analysis of the data on the vapourization processes and thermodynamic properties of cesium-, strontium- and barium compounds at high temperatures is a matter of sustained interest in the European Union and Japan as far as this research is essential for preventing severe accidents on nuclear power plants.[42]

‡ Decree of the President of the Russian Federation No. 642 of December 1, 2016, http://www.kremlin.ru/acts/bank/41449/page/1

V.L.Stolyarova, A.L.Shilov, T.V.Sokolova, M.Kurata, D.Costa
*Russ. Chem. Rev.*, 2023, **92** (5) RCR5059

5 of 22

## 2. The Knudsen effusion mass spectrometry

The power and advantages of the high temperature KEMS and its exceptional capacity for thermodynamic studies of a wide range of inorganic substances have been summarized in a number of monographs and papers, for example, in recent reviews.[1,2] Detailed information on the vapourization processes and partial pressures of vapour species over the binary and multicomponent systems can be obtained by KEMS with the complementary thermodynamic data derived from this information. It should be underlined that these data are of great value in the field of new generation nuclear plants operation and safety researches, including such urgent issues as characterization of newly designed tristructural isotropic (TRISO) nuclear fuels, escape of radioactive components from reactor core melts and during preparation of glass matrixes for disposal of radioactive waste, particularly in the cases when nonvolatile components of glasses have to be used for reducing the activity of radioactive Cs, Sr, Ba contained in them. An account of KEMS as one of the most informative methods of high-temperature chemistry and its attractive features for the thermodynamic studies can be found in survey.[43]

A state-of-the-art description of the method was made by Drowart *et al.*[44] The report outlines principles of the KEMS method, provides a thorough critical analysis of the limits of its applicability and of reliability of the experimental results, and evaluates the methods of the thermodynamic calculations. With reference to the cited report, only a brief summary of the main points characterizing the experimental techniques used in the recently published works investigating the $Cs_2O$-, $SrO$-, and $BaO$-containing oxide systems are given below.

The key element of the method is the effusion cell, that is, a capsule containing the sample under investigation furnished with a small orifice of the area $s$ ($cm^2$) and heated to a required temperature $T$ (K) under high vacuum conditions. For validity of the method the orifice and the temperature should be small enough to ensure that the vapour inside the cell is saturated and can be treated as a perfect gas. Under these conditions the vapour species escape from the cell in the form of a molecular flow for which the kinetic theory of gases gives the equation

$$\frac{dn_j}{dt} = \frac{p_j s C}{(2\pi M_j R T)^{1/2}} \qquad (1)$$

relating the amount $dn_j$ ($mol\ s^{-1}$) of a species $j$ effusing from the cell in the time $dt$ with the partial pressure $p_j$ (Pa) of this species in the cell according to the Hertz–Knudsen equation; here $M_j$ is the molar mass of the species $j$, $R$ is the gas constant, and $C$ is the Clausing factor of the orifice ensuring correction for the actual geometry of the orifice.

The molecular beam cut from the effused flux by a set of slits gets into the ion source and the ionic species generated in it are then sorted by the mass analyzer according to their mass-to-charge ratio $m_i/z_i$. Since the intensity of the $i$-th ion peak in the recorded mass spectrum multiplied by the temperature of the cell is proportional to the amount of the molecular species from which it was formed, equation (1) can be used for determining the partial pressures of the vapour species. However, due to a variety of the possible ionization schemes and coincidence of masses of the different ions the origin of some of the ion peaks cannot be established immediately. For the identification of the molecular precursors of the ions, usually referred to as

deciphering of mass spectra, four main methods were employed in the considered studies:

— measurement of the appearance energy of the ions and recording of the ionization efficiency curves;

— comparison of the intensity of the ion peaks with the isotopic abundance of the constituent elements;

— observation of the effects of variation of the temperature and the composition on the relative intensity of the peaks of ions in mass spectra of vapour;

— measurement of the vapour species in non-saturated vapour enabled by the use of two-temperature double cells.

In all studies mentioned above the electron impact ionization was used. Mass spectra were obtained employing quadrupole mass filters or sector magnetic mass analyzers, the latter characterized by the higher mass resolution. The effusion cells with the sample under study were usually heated by resistance vacuum furnaces or by electron impact techniques.

The partial pressures of vapour species in the reviewed studies were measured according two main approaches, traditionally adhered to in each research group: direct comparison of the ion currents in mass spectra of vapour over the system under study (differential mass spectrometry) and over the reference substance and measurements based on the determination of the device sensitivity constant. In differential mass spectrometry the sample and the reference substance are vapourized in the same experimental run from two cells of the same crucible ('twin-cell'). When individual substance is taken as a reference the value of a component activity can be determined directly as the ratio of the ion currents in mass spectra of vapour over the system under study and over the reference substance. In other cases, the vapour pressure standards had to be used. In many cases determination of the absolute values of partial pressures of vapour species was performed by mass loss measurements based on Eqn (1) that is traditionally called the complete vapourization method.

Two main limitations often experienced in the high-temperature effusion studies of oxide systems were actual also in the studies of these systems containing cesium, strontium, and barium oxides. Strong interaction of the samples under study with the material of effusion cells, that was usually Mo or W, lead to formation of molybdenum and tungsten oxides and had to be taken into account in the consideration of the vapour phase composition and mass balance of the vapourization process. The other hindrance is dissociative vapourization of oxides and hence the presence of oxygen in the vapour over the samples. In most cases the partial pressure of the vapour species cannot be measured and have to be calculated from other vapourization reactions and their equilibrium constants introducing thereby additional uncertainty in the results.

The experimental errors characteristic of the KEMS method in general are scrutinized in report[43] in all aspects. The given analysis indicates that there are more than a dozen factors that can reduce significantly the reliability of the results, but the most serious one considered in every detail in Ref. 44 is the ionization cross-sections of complex vapour species and methods of their assessment.

Depending on the available experimental and reference data, their quality and abundance, the thermochemical data in the considered studies were obtained by application of the second law of thermodynamics based on the equation

$$\Delta H_r^\circ(T) = -R\ \frac{d\ln K_p(T)}{d(1/T)} \qquad (2)$$

where $K_p$ is the equilibrium constant calculated using the partial pressure of the reaction under consideration, or by application of the third law of thermodynamics using the equation

$$-RT \ln K_p = \Delta H_r^\circ(T) - T\Delta S_r^\circ(T) \qquad (3)$$

or, in many cases, by both of these methods. Analysis given in Ref. 44 shows that none of these methods is definitely preferable and only good agreement between the results can indicate that possible systematic errors are under control.

All approaches in the KEMS studies nowadays are mostly the traditional ones [1, 8, 9] but nevertheless further improvement of the experimental techniques goes on as it is shown, for example, in Ref. 45.

# 3. The Cs-bearing systems

The HTMS studies of the 50s and 60s were focused on revealing the capabilities of this method, its further development, and re-assessment of the existing total vapour pressure data using mass spectrometric information on molecular species in the vapour and their partial pressures. In the next two decades the efforts were devoted largely to comparative studies of volatility and thermodynamic properties in groups of substances, such as oxides, halides, and gaseous salts, and establishing regularities of their transformation imposed by the position of their constituent elements in the Periodic Table. In the 80s and 90s, much attention was paid also to investigations of the high-temperature properties of materials having practical application, such as glasses, ceramics, high-temperature construction and nuclear engineering materials, and to acquisition of the data for thermodynamic modeling.

One of the most important problems where the HTMS data are required is obtaining detailed knowledge of volatility of materials used in nuclear energetics and formed in heavy accidents in NPPs. Volatile components, which can be released to the environment during reactor core melting and other environmentally hazardous processes and lead to transport and spreading of the radioactive waste, were studied in a considerable number of research works of the last four decades, especially in a series of systematic studies of the vapourization processes and thermodynamic properties of alkali oxides, alkali earth oxides, and multicomponent melts and glasses bearing them. In view of the possible dissipation routes of radioactive species, of particular interest in the study of the vapour phase is the formation of gaseous associates and methods of their identification by HTMS methods.

Thus, a vast amount of mass spectrometric information on the vapourization behaviour and thermodynamic properties of oxide systems containing oxides of the first and second groups of the Periodic Table including $Cs_2O$, SrO, and BaO have been accumulated up to date. The studies of the last two decades in this field were aimed at acquisition of more reliable, accurate, or complete information on the earlier investigated systems, obtaining data on the yet unexplored ones, modelling their thermodynamic properties, and search of criteria of stability of various molecular species in the vapour. The latter objective depends most critically on the completeness and diversity of the database making significant additional research on any kind of oxide systems. Consider first the most interesting recent studies of the cesium oxide-bearing systems.

## 3.1. The Cs−O−H system

In severe nuclear accidents, cesium and iodine are the main gaseous fission products that can be transported with steam and condensed water and with such products of their reactions as cesium hydroxide. As a part of the French program to study the behaviour of iodine in components of the reactor core melt (corium) during these accidents, HTMS investigation of the pseudo-binary CsI−CsOH system was undertaken by Roki *et al.*[46−48]

Its first part[46] was a mass spectrometric study of the CsOH(s,l) vapourization processes. It was aimed at interpretation of the available total vapour pressure data provided by transpiration method, clarification of the earlier obtained KEMS method results, and to determining the dissociation enthalpy of dimeric cesium oxide vapour species. It was also intended to check the used reference data, which had been derived from a highly scattered experimental data.

The highest attainable quality of the obtained experimental data was set as a goal that had to be achieved as a result of most careful preparation of the samples, improved manipulation of molecular beams, eliminating possible sample creeping and surface diffusion effects, detailed consideration of the ionization processes and mass spectrometric results. Special modifications of the apparatus had been made in order to improve the reliability of the measurements referring to collimation of the molecular beam, the shutter system, and the ionization chamber. The study[46] provides an example of highly refined HTMS techniques and demonstrates the attainable efficiency of the method.

It was established[46] that the vapour over CsOH(s,l) in the temperature range 500−770 K consists of the monomer CsOH and the dimer $Cs_2O_2H_2$ gaseous species. Analysis of the appearance energies of the recorded ions in mass spectra of vapour over CsOH proved that the observed the $Cs_3O_2H^+$ and $Cs_3O_2H_2+$ ions were the products of dissociative ionization of the trimer gaseous molecule $Cs_3O_3H_3$. The two main independent reactions that were used for calculations of the thermodynamic data according to the 3rd law treatment were the following:

$$CsOH(s,l) = CsOH(g), \qquad (4)$$

$$\Delta H_{diss}^\circ(298\ K) = (163.3 \pm 6.5)\ kJ\ mol^{-1}$$

$$Cs_2O_2H_2(g) = 2\,CsOH(g), \qquad (5)$$

$$\Delta H_s^\circ(298\ K) = (146.6 \pm 7.3)\ kJ\ mol^{-1}$$

A thorough analysis of all possible errors specific for the treatment of the obtained experimental data according to the 2nd and 3rd laws of thermodynamics indicated that the latter, as it is stated in most cases, provides more reliable values.

Taking into account that cesium hydrate is a substance rather laborious for the vapour phase investigations and that the authors[46] performed the study at the highest attainable level the uncertainties given in (4) and (5) can be regarded as a lower limit of HTMS accuracy at present.

The next stage of the project included a study of the vapour phase over the Cs−I−O−H system using the results obtained for the CsOH (Ref. 46) and CsI systems. Mass spectrum of the vapour over the samples of the quasi-binary CsI−CsOH system evaporated from the Knudsen cell in the temperature range 657−863 K was recorded. Monomers and dimers of cesium hydrate and iodide, and their associated forms, which had to be identified, in most part ionized with dissociation yielding similar or indistin-

V.L.Stolyarova, A.L.Shilov, T.V.Sokolova, M.Kurata, D.Costa
*Russ. Chem. Rev.*, 2023, **92** (5) RCR5059

7 of 22

guishable by $m/z^+$ ions. Therefore, deciphering of the mass spectra required analysis of variation of ion peak ratios as a function of the sample composition and temperature. Composition of the vapour over the system determined from the mass spectral data confirmed that in addition to monomers and dimers a complex gaseous species existed in the vapour that was formed as a result of the gas phase reaction

$$CsI(g) + CsOH(g) = Cs_2IOH(g) \qquad (6)$$
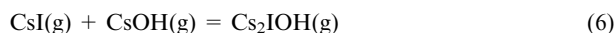
the standard enthalpy of formation for which was determined using the 3rd law of thermodynamics as $\Delta H_f^\circ(298 \text{ K}) = (-578 \pm 14.7) \text{ kJ mol}^{-1}$.

## 3.2. CsBO$_2$

In nuclear reactors containing large amounts of boron, severe reactor accidents may lead to formation of gaseous cesium metaborate according to reaction:

$$CsI(g) + H_3BO_3(g) \longrightarrow CsBO_2(g) + HI(g) + H_2O(g), \qquad (7)$$

as one of the main cesium-bearing vapour species. Nakajima *et al.*[49] considered that the available thermodynamic data on $CsBO_2(g)$ is poor for accurate analysis of reaction (7) and should be re-assessed. The objective of their study was to improve the reliability of the existing thermodynamic data by performing more accurate Knudsen effusion mass spectrometric measurements including: vapourization from platinum effusion cell, scrupulous chemical and structural analysis of the samples, and thorough evaluation of the experimental errors.

Mass spectra of the vapour over $CsBO_2$ recorded with a quadrupole mass spectrometer were in agreement with the literature data and confirmed the presence of dimeric $Cs_2B_2O_4$ gaseous molecule in vapour. However, its small ($<1\%$) concentration in the vapour was not taken into account in further consideration though all results of the study were obtained actually by mass-loss measurements. The analyses of the condensed phase composition indicated that after vapourization runs in the temperature range $792-915$ K the concentration of $B_2O_3$ in the samples became 1 mol.% higher, which meant that the vapourization process was not strictly congruent.

The values of the standard enthalpy of formation of $CsBO_2(g)$, obtained by the 2nd and 3rd law treatment, were $-(700.7 \pm 10.7)$ and $-(697.0 \pm 10.6)$ kJ mol$^{-1}$, respectively, in reasonable agreement with values reported in earlier publications. The authors concluded that, contrary to their assumptions, the reliability of the thermodynamic data obtained in their KEMS study[49] was comparable to the reliability of the data derived from the $CsBO_2(g)$ molecular constants.

## 3.3. The Cs$_2$O — B$_2$O$_3$ system

For analysis of the corium radioactive emission and developing techniques of radioactive waste vitrification, understanding the vapourization processes of the cesium-boron oxide system is one of the primal issues. The data on the vapour phase over samples of the $Cs_2O-B_2O_3$ system obtained in Ref. 50 gives some idea of a variety of results that can be obtained by the HTMS method. Samples of the melts containing from 0.05 to 0.5 mole fractions of $Cs_2O$ were vapourized from molybdenum twin cells using differential mass spectrometric approach in the temperature range of $1020-1100$ K and the recorded mass spectra of effusing vapour over this system were analyzed with the help of the additionally measured ionization efficiency curves. Cesium metaborate $CsBO_2$ was taken as a reference

since it had been established[50] that $CsBO_2(l)$ evaporates in the form of monomer $CsBO_2(g)$ without significant dissociation. Concentration of $(CsBO_2)_2$ dimer did not exceed $3-5\%$ and at higher temperatures, Cs(g) could also be identified in the vapour in a negligible concentration.

The vapour over the $Cs_2O-B_2O_3$ system was nearly the same as over cesium metaborate. Boron oxide is less volatile than $CsBO_2$ and therefore, the surface layer should be enriched with $B_2O_3$, thereby modifying the actual vapourizing composition to some extent.

The presence of $Cs_2B_2O_4$ in the vapour made possible application of the monomer-dimer equilibrium method for the determination of the component activities. Since obtaining the data on the $CsBO_2$ activity in the $CsBO_2-B_2O_3$ system from the ion currents measured for monomer and dimeric vapour species available in mass spectra of vapour over the system under study and $CsBO_2$ does not require knowledge of ionization cross-sections of gaseous molecules or conversion coefficients of secondary electron multiplier, the most serious sources of errors were eliminated. First, the system was treated in terms of $CsBO_2$ and $B_2O_3$ components. The $B_2O_3$ activity values as a function of concentration in the $CsBO_2-B_2O_3$ system were determined by the Gibbs–Duhem equation. From the resulting Gibbs formation energy ($\Delta G$) in the $CsBO_2-B_2O_3$ system and reference data for the standard Gibbs energy of the $CsBO_2$ formation the thermodynamic functions for the $Cs_2O-B_2O_3$ system were calculated, Table 1, indicating that the system under study is characterized by strong negative deviation from the ideal behaviour.
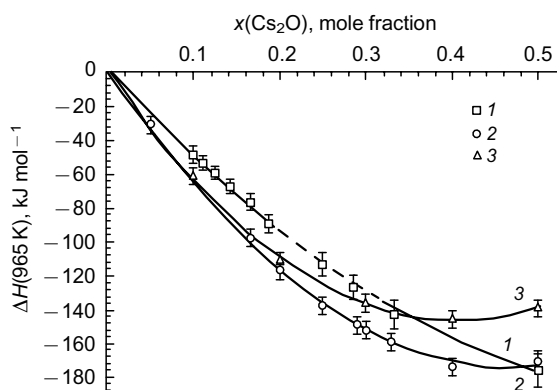
The component activities and the Gibbs energies of formation in the $Cs_2O-B_2O_3$ melt were optimized in the study[50] using statistical thermodynamics model based on the generalized lattice theory of associated solutions (GLTAS). The main purpose of such modeling was evaluation of the relative numbers of bonds of different types in the melt to get additional insight into the thermodynamic properties of the system. The number of input points, Table 1, made possible the computation of a clearly defined interpolation curves that demonstrated a fairly good agreement with the experimental values of the $Cs_2O$ activities and rather poor agreement in case of $B_2O_3$. The conformity was improved considerably by application the vacancy type of model in which an additional contact point ('vacancy') was attributed to the $Cs_2O$ structural unit of the lattice. Cesium oxide, which plays the role of a glass modifier in $Cs_2O-B_2O_3$ melt, should produce the effect of breaking the boron oxide network in the model lattice and therefore introduction of the 'vacancy bond' enables better optimization. The method was successfully used further in optimi-

**Table 1.** The chemical potentials of components ($\Delta\mu_i$) and the Gibbs energy of formation in the $Cs_2O-B_2O_3$ system[50] at the temperature 1020 K.

| Sample composition, mole fractions | | $-\Delta\mu(B_2O_3)$, kJ mol$^{-1}$ | $-\Delta\mu(Cs_2O)$ kJ mol$^{-1}$ | $-\Delta G$ kJ mol$^{-1}$ |
|---|---|---|---|---|
| Cs$_2$O | B$_2$O$_3$ | | | |
| 0.05 | 0.95 | 0 | 451.0 | 43.6 |
| 0.10 | 0.90 | 0.9 | 428.2 | 22.5 |
| 0.20 | 0.80 | 0.5 | 419.5 | 84.3 |
| 0.25 | 0.75 | 0.4 | 416.0 | 104.3 |
| 0.33 | 0.67 | 1.2 | 409.3 | 137.9 |
| 0.40 | 0.60 | 14.7 | 383.0 | 162.0 |

8 of 22

V.L.Stolyarova, A.L.Shilov, T.V.Sokolova, M.Kurata, D.Costa
*Russ. Chem. Rev.*, 2023, **92** (5) RCR5059

zation of the other systems containing glass oxide-modifiers.

Further study of the $Cs_2O-B_2O_3$ system [51] showed that the main vapour species over this system were $CsBO_2$ and $Cs_2B_2O_4$, their partial pressures were obtained. The Gibbs energies of formation, the excess Gibbs energies, the partial mole enthalpies of mixing, and total enthalpies of mixing were determined in the $Cs_2O-B_2O_3$ system as functions of temperature in the range $789-1215$ K. When comparing the obtained data [51] with the values found earlier, [52-54] their mutual agreement was successfully illustrated (Figs $5-7$) using various approaches including the electromotive force (EMF) method. [54]

### 3.4. The $Cs_2O-B_2O_3-SiO_2$ system

Thermodynamic properties of glasses and melts in the $Cs_2O-B_2O_3-SiO_2$ system were studied in detail in Refs $55-58$ in connection with the problem of utilization of radioactive waste by vitrification in borosilicate matrixes. Compositions of the samples synthesized for this study are listed in Table 2. The experimental procedure to study vapourization processes and thermodynamic properties was similar to the one described earlier. [50] Complex analysis of the mass spectral data obtained indicated that the main vapour species over $Cs_2O-B_2O_3-SiO_2$ melts in the temperature range of $995-1110$ K were the $CsBO_2$ monomers with a minor admixture of the $(CsBO_2)_2$ dimers. The $CsBO_2$ activities in $Cs_2O-B_2O_3-SiO_2$ melts were obtained according to the similar approach as in Ref. 50 using the monomer and dimer ratio method (see Table 2).

It was concluded that the main vapourization process of samples No $1-4$, 7 could be described according to the reaction:

$$3CsBO_2(l) \longrightarrow CsBO_2(g) + Cs_2B_2O_4(g) \qquad (8)$$

and in the case of samples Nos 5, 6, $8-10$ the additional vapourization reaction contributes significantly:

$$Cs_2SiO_3(s,l) = 2Cs(g) + 0.5O_2 + SiO_2(s) \qquad (9)$$

In the concentration range of samples Nos $6-11$, Table 2, the ternary $Cs_2O-B_2O_3-SiO_2$ system could be considered as a quasi-binary $CsBO_2-Cs_2SiO_3$ system. In this case the $CsBO_2$ activities were measured directly, whereas the $Cs_2SiO_3$ activities were calculated using the Gibbs-Duhem equation. It should be underlined that the deviations from the ideal behaviour of the excess Gibbs energy obtained in glasses and melts of quasi-binary $CsBO_2-Cs_2SiO_3$ system as a function of concentration change its sign at the composition about 0.65 mole fraction of $CsBO_2$.

The obtained excess Gibbs energy functions were used in the theoretical study [56, 58] to illustrate the high potential capability of the GLTAS in optimization and prediction of

**Figure 5.** The enthalpy of mixing in the $Cs_2O-B_2O_3$ system obtained at the temperatures 965 K (*1*) [51] and at 800 K (*2*) [51] as well as at 1200 K (*3*). [54]

**Figure 6.** The Gibbs energies of formation in the $Cs_2O-B_2O_3$ system at 800 K. *1* shows the results, [51] *2* is the data obtained by the EMF method by Kozhina and Shultz. [54]
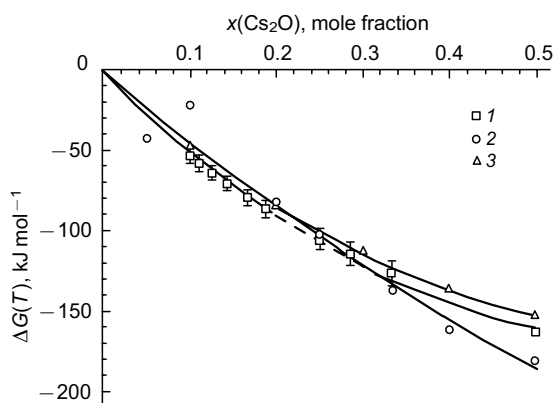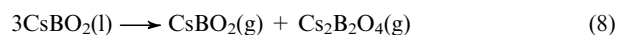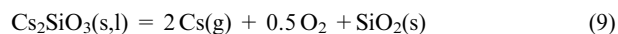
**Figure 7.** The Gibbs energies of formation in a $Cs_2O-B_2O_3$ system. *1* shows the results published in Ref. 51 at a temperature of 1000 K; *2* is the result obtained by the high-temperature mass spectrometric method by Stolyarova *et al.* [50] at a temperature of 1020 K; *3* is the data obtained by the EMF method by Kozhina and Shultz [54] at a temperature of 1200 K.

**Table 2.** The $CsBO_2$ activities, $a(CsBO_2)$, in $Cs_2O-B_2O_3-SiO_2$ melts, at a temperature of 1020 K. [55]

| No | Composition, mol.% | | | Estimated phase composition, mol.% | | | | $a(CsBO_2)$ |
|----|------|------|------|-------|------|------|---------|------------|
| | $Cs_2O$ | $B_2O_3$ | $SiO_2$ | $CsBO_2$ | $B_2O_3$ | $SiO_2$ | $Cs_2SiO_3$ | |
| 1 | 6 | 56 | 38 | 12 | 50 | 38 | — | $8 \times 10^{-3}$ |
| 2 | 10 | 54 | 36 | 20 | 44 | 36 | — | 0.01 |
| 3 | 20 | 48 | 32 | 40 | 28 | 32 | — | 0.06 |
| 4 | 33.3 | 40 | 26.7 | 66.7 | 6.6 | 26.7 | — | 0.29 |
| 5 | 40 | 36 | 24 | 75 | — | 20.8 | 4.2 | 0.78 |
| 6 | 50 | 30 | 20 | 75 | — | — | 25 | 0.84 |
| 7 | 50 | 50 | — | 100 | — | — | — | 1.0 |
| 8 | 50 | 40 | 10 | 88.9 | — | — | 11.1 | 0.88 |
| 9 | 50 | 20 | 30 | 57.1 | — | — | 42.9 | 0.81 |
| 10 | 50 | 10 | 10 | 33.3 | — | — | 66.7 | 0.67 |
| 11 | 50 | — | 50 | — | — | — | 100 | 0 |

V.L.Stolyarova, A.L.Shilov, T.V.Sokolova, M.Kurata, D.Costa
*Russ. Chem. Rev.*, 2023, **92** (5) RCR5059

9 of 22

the thermodynamic properties of oxide systems taking the $Cs_2O-B_2O_3-SiO_2$ system as an example, so that previously obtained results could be analyzed and developed. Since the $Cs_2O-B_2O_3-SiO_2$ system is formed by two glass-forming and one glass-modifying oxide, the vacancy modification of the model was applied: one additional contact point generating 'vacancy' bonds was assigned to the $Cs_2O$ structural unit. The accepted model and the calculation procedure were analogous to those used in earlier works on optimization of oxide systems. The values of a part of the adjustable energy parameters used for the calculations were taken the same as in the earlier optimized lattice models of the glasses and melts in the $Na_2O-SiO_2$, $B_2O_3-SiO_2$, and $Cs_2O-B_2O_3$ systems. It proves that optimization on the basis of GLTAS in some cases may be useful for prediction of thermodynamic properties of multicomponent systems when some common set of parameters obtained for their constituent subsystems can be chosen.[56]

The Gibbs energy functions in the $Cs_2O-B_2O_3-SiO_2$ system optimized in [56] in the frame of the GLTAS approach were compared with the experimental data and with $\Delta G$ functions constructed using the Wagner method. All these functions were found to be in reasonable agreement.

Finally, interrelation between the thermodynamic properties of glasses and melts in the $Cs_2O-B_2O_3-SiO_2$ system and their specific structural features were discussed in Ref. 56 using the calculated concentration dependencies of the relative number of bonds of different types when the second coordination sphere of atoms was taken into consideration.

To verify the consistency of the thermodynamic data obtained in the $Cs_2O-B_2O_3-SiO_2$ system they were compared [59] with similar results obtained for a series of ternary silicate systems such as the $MgO-Al_2O_3-SiO_2$, $CaO-Al_2O_3-SiO_2$, $CaO-TiO_2-SiO_2$, and $BaO-TiO_2-SiO_2$ systems. In contrast to the $Cs_2O-B_2O_3-SiO_2$ system comprising one oxide-modifier there are two modifying oxides in all these silicate systems. It was interesting to check the validity of optimization based on the GLTAS approach when two types of vacancies are introduced into the model lattice. The parameters of the lattice model chosen as a basis for optimization may serve as certain analogues of the chemical bonds in the real melts and glasses in the system under study and thus may illustrate the relation between the observed deviations of the thermodynamic functions from ideality and the corresponding changes in the relative number of bonds of different types. Therefore, a possibility of interpretation of model parameters in terms of a corresponding real melt structure was a matter of concern in the survey [59] and other studies dealing with the GLTAS-based optimization.

The results of modeling indicated that glasses and melts in the systems with oxides of elements of the second group of the Periodic Table could also be beneficially optimized within the frame of the GLTAS approach and that the interpolated thermodynamic functions were generally within the uncertainty limits of the results that may be obtained using the HTMS method.

### 3.5. The $Cs_2O-Al_2O_3-SiO_2$ system
From the point of view of consequences for the final storage of high-level radioactive waste vapourization of the synthetic compounds formed in the $Cs_2O-Al_2O_3-SiO_2$ system such as $CsAlSiO_4$, $CsAlSi_5O_{12}$ and $CsAlSi_2O_6$ was studied by KEMS up to the temperature of 1803 K.[60] It was found that Cs was the main vapour species over

these compounds. The following values of enthalpies of the Cs sublimation were obtained such as $\Delta H^{\circ}_{s,1495}(CsAlSiO_4) = (356.6 \pm 9.8)$ kJ mol$^{-1}$ and $\Delta_s H^{\circ}_{s,1673}(CsAlSi_5O_{12}) = (516.3 \pm 18.0)$ kJ mol$^{-1}$.
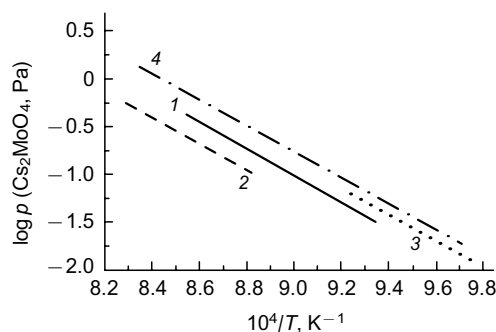
### 3.6. $Cs_2MoO_4$
Kazenas *et al.*[61] observed cesium molybdate sublimation from platinum effusion cells in the temperature range of $1026-1148$ K. The vapour phase was studied using traditional approaches. Only the $Cs^+$ and $Cs_2MoO_4^+$ ions were identified in the mass spectrum of vapour over $Cs_2MoO_4$. Appearance energies of the ions in the mass spectrum of vapour over $Cs_2MoO_4$ showed that $Cs^+$ was a fragment ion and $Cs_2MoO_4^+$ was a molecular ion. During a complete isothermal vapourization, the ion currents of vapour species in the mass spectrum of vapour over $Cs_2MoO_4$ were nearly constant proving that the vapourization process was congruent. Absolute values of the $Cs_2MoO_4$ partial vapour pressure were determined *via* the sensitivity constant of the mass spectrometer and its temperature dependence could be expresses by the equation

$$\log p(Cs_2MoO_4, atm) = -13724/T + 6.47 \qquad (10)$$

To predict possible processes during the operation of NPP, it is of considerable interest to study the $Cs_2O-MoO_3$ system. In the recent study of this system [62] a number of thermodynamic characteristics have been obtained as a function of temperature such as the component activities, the Gibbs energies of formation and the excess Gibbs energies. Furthermore, some values such as the $MoO_3$ and $Cs_2MoO_4$ partial molar enthalpies of mixing, the $Cs_2MoO_4$ partial vapourization enthalpy, and the total enthalpy of mixing in the $Cs_2O-MoO_3$ system were found for the first time. It is shown that the main vapour species over the system under study are $MoO_3$, $Mo_2O_6$, $Mo_3O_9$, $Mo_4O_{12}$ and $Mo_5O_{15}$. In addition to the HTMS method, various physicochemical methods were also used for the samples identification.[62] Fig. 8 summarizes the available data on the dependences of decimal logarithms of the $Cs_2MoO_4$ partial pressures over $Cs_2MoO_4$ on reverse temperature according to Refs 62–65.

### 3.7. $Cs_2WO_4$
Mass spectrometric study of the $Cs_2WO_4$ vapourization [66] confirmed that in the temperature range of $1017-1200$ K cesium tungstate vapourizes mainly congruently. The assessed enthalpy of $Cs_2WO_4(g)$ atomization could be fairly



**Figure 8.** The dependences of decimal logarithms of the $Cs_2MoO_4$ partial vapour pressures over $Cs_2MoO_4$ on reverse temperature. *1* is the result obtained in Ref. 63 (solid line), *2* is the result obtained in Ref. 64 (dashed line), *3* is the data found in Ref. 65 (dotted line), and *4* is the data found in Ref. 62 (dash-dotted line).

10 of 22

V.L.Stolyarova, A.L.Shilov, T.V.Sokolova, M.Kurata, D.Costa
*Russ. Chem. Rev.*, 2023, 92 (5) RCR5059

well described as the linear dependence from the atomization enthalpy of the gaseous anion-forming oxide.

Kazenas *et al.*[67] reported the similar results in which no new features in the process of cesium tungstate vapourization were found.

### 3.8. Cs$_2$SeO$_4$

Vaporization of Cs$_2$SeO$_4$ was studied by KEMS[68] and the following sublimation processes were observed:

$$Cs_2SeO_4(s) = Cs_2SeO_4(g) \tag{11}$$

$$Cs_2SeO_4(s) = Cs_2SeO_3(s) + 0.5\,O_2 \tag{12}$$
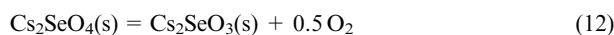
It should be mentioned that at the increasing temperature dissociation of Cs$_2$SeO$_4$(g) was preferable.

## 4. The Sr-bearing systems

Originally, vapourization and thermodynamic properties of strontium and barium oxides were studied for the purpose of development of oxide cathode used in electronic tubes and hence of particular interest were such properties as electronic and thermionic emission and mass loss rate of SrO-coated filaments. Later study of SrO volatility was connected with the problem of the dissipation of the radioactive strontium formed in severe accidents on nuclear power plants or contained in glass matrixes used for the isolation of radioactive wastes from the environment, for which purposes borosilicate glasses are most often used.

Thus, a lot of information on the volatility of strontium oxide has been reported already and the only recent examination[69] of the vapour phase over pure SrO were made in course of the study of the vapourization processes of the SrO$-$SiO$_2$ system that required some auxiliary data. Strontium oxide was vapourized from a molybdenum cell at a temperature of 1983 K at the ionization energy 25 eV. The following ions were identified in the mass spectrum of vapour over SrO such as Sr$^+$, SrO$^+$, SrMoO$_4^+$, SrMoO$_3^+$, MoO$_3^+$, MoO$_2^+$. Determination of the appearance energies of the ions in mass spectrum of vapour over SrO allowed to conclude that SrO and Sr were the main gaseous species over SrO. Their partial pressures were measured by the method of comparison of ion currents using gold as the partial vapour pressure standard. The partial pressures of the SrO and Sr vapour species as a function of temperature required for the further thermodynamic calculation were expressed by the following equations:[69]

$$\log p(\text{SrO, atm}) = -(28121 \pm 830)/T + (7.47 \pm 0.17) \tag{13}$$

$$\log p(\text{Sr, atm}) = -(2195 \pm 654)/T + (6.59 \pm 0.08) \tag{14}$$

Since the major part of the results considered below were obtained using the same experimental procedure as in the cited study,[69] only special details of mass spectral techniques will be mentioned in the further discussion.

### 4.1. The SrO$-$B$_2$O$_3$ system

The pioneering studies of vapourization processes and thermodynamic properties of compounds available in the condensed phase of the SrO$-$B$_2$O$_3$ system such as 2 SrO·B$_2$O$_3$, SrO·B$_2$O$_3$ and SrO·2 B$_2$O$_3$ were carried out by Asano and Kou[70–78] by KEMS. Variation of the Sr, SrBO$_2$, BO, BO$_2$, B$_2$O$_3$ and B$_2$O$_2$ partial vapour pressures with increase of the B$_2$O$_3$ content in the condensed phase of the SrO$-$B$_2$O$_3$ system in the temperature range of 1282$-$1572 K according to Ref. 70 is presented in Table 3.

**Table 3**. Variation of the Sr, SrBO$_2$, BO, BO$_2$, B$_2$O$_3$ and B$_2$O$_2$ partial vapour pressures with increase of the B$_2$O$_3$ content in the condensed phase of the SrO$-$B$_2$O$_3$ system in the temperature range of 1282$-$1572 K according to Asano and Kou.[70]

| Vapour species | Composition of the condensed phase | | |
|---|---|---|---|
| | 2 SrO·B$_2$O$_3$ | SrO·B$_2$O$_3$ | SrO·2 B$_2$O$_3$ |
| Sr | > [a] | ≈ [b] | ≈ |
| SrBO$_2$ | < [c] | < | < |
| BO | < | < | < |
| BO$_2$ | < | < | < |
| B$_2$O$_2$ | < | < | < |
| B$_2$O$_3$ | < | < | < |

[a] The symbol $>$ indicates an increase in the corresponding partial pressure of the vapor species as a function of the concentration of boron oxide in the condensed phase. [b] The symbol $\approx$ indicates the approximate independence of the partial pressure of the vapor species as a function of the concentration of boron oxide in the condensed phase. [c] The symbol $<$ indicates a decrease in the corresponding partial pressure of the vapor species as a function of the concentration of boron oxide in the condensed phase.

Equations for the partial vapour pressures of species as a function of temperature over the SrO$-$B$_2$O$_3$ system as well as enthalpies of formation for strontium borates from elements and from constituent oxides are presented in Tables 4 and 5 according to Refs 70$-$78.

Later, the study[79] showed that the SrB$_2$O$_4$ vapourization from molybdenum effusion cells in the temperature range 1500$-$1600 K proceeded according to the following reactions:

$$SrB_2O_4(l) = SrB_2O_4(g) \tag{15}$$

$$SrB_2O_4(l) = SrO(s) + B_2O_3(g) \tag{16}$$
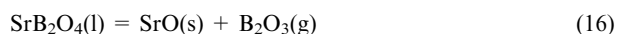
At higher temperatures, as the condensed phase was enriched with strontium oxide, only the SrBO$_2$, SrO, and BO species were identified in the vapour. Their partial pressures in the temperature range of 2141$-$2272 K and the equilibrium constant of gas-phase reaction

$$SrBO_2(g) = SrO(g) + BO(g) \tag{17}$$
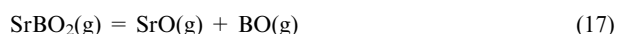
were determined. As a result, the following thermodynamic values were found:

— enthalpy of SrB$_2$O$_4$(l) vapourization, $\Delta H_{v,298}^{\circ} = 591.4$ kJ mol$^{-1}$;

— standard enthalpies of SrB$_2$O$_4$(g) and SrBO$_2$(g) formation, $\Delta H_{f,298}^{\circ} = -1425$ and $-571.0$ kJ mol$^{-1}$, respectively, and

— standard enthalpy of SrB$_2$O$_4$(g) and SrBO$_2$(g) atomization, $\Delta H_{at,298}^{\circ} = 3712$ and 1795 kJ mol$^{-1}$, respectively.

A number of valuable characteristics of borate glasses, such as intense absorption of slow neutrons and low absorption of X-rays, motivated the HTMS study[80] of the vapourization processes and thermodynamic properties in SrO$-$B$_2$O$_3$ melts. The component activities in the SrO$-$B$_2$O$_3$ system were obtained at a temperature range of 1500$-$1650 K. According to the phase diagram the region of melts at these low temperatures extends from 0 to 66.3 mol.% of SrO. Nine samples with compositions in this concentration range were studied and vapourized from molybdenum effusion cells.

Mass spectral analysis of the vapour over the samples relied heavily on the results of study[79] and led to a conclusion that there were no other species in the vapour

V.L.Stolyarova, A.L.Shilov, T.V.Sokolova, M.Kurata, D.Costa
*Russ. Chem. Rev.*, 2023, **92** (5) RCR5059

11 of 22

**Table 4**. The partial vapour pressures of species as a function of temperature over the $SrO-B_2O_3$ system according to Refs 70, 75, 78.

| Composition of condensed phase | Vapour species | Tempe-rature, K | $\log p_i(Torr) =$ $-A \times 10^{-3}/T + B$ | | Ref. |
|---|---|---|---|---|---|
| | | | $A \times 10^{-3}$ | $B$ | |
| $2\,SrO \cdot B_2O_3$ | Sr | 1452 – 1572 | $23.93 \pm 1.00$ | $10.00 \pm 0.66$ | 70 |
| | $SrBO_2$ | 1452 – 1572 | $28.18 \pm 1.45$ | $13.74 \pm 0.96$ | |
| | BO | 1473 – 1572 | $22.34 \pm 0.68$ | $9.79 \pm 0.45$ | |
| | $BO_2$ | 1473 – 1572 | $29.95 \pm 0.86$ | $11.33 \pm 0.57$ | |
| | $B_2O_2$ | 1473 – 1572 | $23.03 \pm 1.03$ | $11.05 \pm 0.68$ | |
| | $B_2O_3$ | 1453 – 1572 | $23.85 \pm 0.73$ | $10.88 \pm 0.48$ | |
| $SrO \cdot B_2O_3$ | Sr | 1373 – 1442 | $32.30 \pm 1.48$ | $15.32 \pm 1.05$ | 70 |
| | $SrBO_2$ | 1310 – 1442 | $30.80 \pm 0.53$ | $16.06 \pm 0.38$ | |
| | BO | 1310 – 1442 | $21.21 \pm 0.35$ | $10.10 \pm 0.26$ | |
| | $BO_2$ | 1310 – 1442 | $32.78 \pm 0.38$ | $14.36 \pm 0.27$ | |
| | $B_2O_2$ | 1310 – 1442 | $19.34 \pm 0.49$ | $9.85 \pm 0.35$ | |
| | $B_2O_3$ | 1310 – 1442 | $25.31 \pm 0.28$ | $13.91 \pm 0.20$ | |
| $SrO \cdot 2\,B_2O_3$ | Sr | 1304 – 1440 | $25.60 \pm 0.58$ | $10.59 \pm 0.42$ | 70 |
| | $SrBO_2$ | 1304 – 1440 | $24.92 \pm 0.28$ | $12.46 \pm 0.20$ | |
| | BO | 1281 – 1440 | $20.75 \pm 0.27$ | $9.79 \pm 0.20$ | |
| | $BO_2$ | 1281 – 1440 | $28.97 \pm 0.16$ | $12.24 \pm 0.12$ | |
| | $B_2O_2$ | 1281 – 1440 | $19.83 \pm 0.19$ | $11.02 \pm 0.14$ | |
| | $B_2O_3$ | 1281 – 1440 | $22.00 \pm 0.42$ | $12.82 \pm 0.31$ | |
| $3\,BaO \cdot B_2O_3$ | Ba | 1434 – 1630 | $21.41 \pm 0.86$ | $7.40 \pm 0.56$ | 75 |
| | $BaBO_2$ | 1434 – 1630 | $23.04 \pm 1.46$ | $9.10 \pm 0.30$ | |
| | BO | 1434 – 1630 | $11.41 \pm 0.33$ | $2.88 \pm 0.22$ | |
| | $BO_2$ | 1434 – 1630 | $27.12 \pm 0.33$ | $8.79 \pm 0.22$ | |
| | $B_2O_2$ | 1434 – 1630 | $11.57 \pm 0.31$ | $3.95 \pm 0.20$ | |
| | $B_2O_3$ | 1434 – 1630 | $10.95 \pm 0.27$ | $1.92 \pm 0.18$ | |
| $BaO \cdot B_2O_3$ | Ba | 1333 – 1535 | $22.48 \pm 0.34$ | $8.40 \pm 0.24$ | 78 |
| | $BaBO_2$ | 1333 – 1535 | $23.26 \pm 0.87$ | $11.73 \pm 0.60$ | |
| | BO | 1389 – 1535 | $17.83 \pm 1.34$ | $7.38 \pm 0.91$ | |
| | $BO_2$ | 1389 – 1535 | $29.69 \pm 1.07$ | $12.43 \pm 0.73$ | |
| | $B_2O_2$ | 1389 – 1535 | $16.95 \pm 1.17$ | $7.75 \pm 0.80$ | |
| | $B_2O_3$ | 1389 – 1535 | $21.64 \pm 1.04$ | $11.21 \pm 0.72$ | |
| $BaO \cdot 2\,B_2O_3$ | Ba | 1277 – 1431 | $25.29 \pm 0.49$ | $10.14 \pm 0.37$ | 78 |
| | $BaBO_2$ | 1277 – 1431 | $25.65 \pm 0.22$ | $13.24 \pm 0.17$ | |
| | BO | 1277 – 1431 | $17.84 \pm 0.71$ | $8.08 \pm 0.53$ | |
| | $BO_2$ | 1277 – 1431 | $32.20 \pm 0.78$ | $14.67 \pm 0.58$ | |
| | $B_2O_2$ | 1277 – 1431 | $15.42 \pm 0.39$ | $9.39 \pm 0.29$ | |
| | $B_2O_3$ | 1277 – 1431 | $22.07 \pm 0.68$ | $12.66 \pm 0.51$ | |

**Table 5**. Enthalpies of formation for strontium- and barium borates from elements and from constituent oxides.[75]

| Borate | $\Delta H^\circ_{f,298}$, kJ mol$^{-1}$ | $\Delta H^\circ_{f,ox,298}$, kJ mol$^{-1}$ |
|---|---|---|
| $[SrO \cdot B_2O_3]$ | $-2016.7 \pm 28.5$ | $-152.8 \pm 28.8$ |
| $[SrO \cdot 2\,B_2O_3]$ | $-3336.5 \pm 20.3$ | $-196.7 \pm 20.0$ |
| $[3\,BaO \cdot B_2O_3]$ | $-3468.6 \pm 49.7$ | $-552.4 \pm 50.1$ |
| $[BaO \cdot B_2O_3]$ | $-1972.3 \pm 28.0$ | $-152.3 \pm 28.2$ |
| $[BaO \cdot 2\,B_2O_3]$ | $\begin{cases} -3331.1 \pm 27.4 \\ -3347.1 \pm 20.5 \end{cases}$ | $\begin{cases} -239.2 \pm 27.4 \\ -255.2 \pm 20.0 \end{cases}$ |

over the $SrO-B_2O_3$ system except gaseous $SrB_2O_4$ and $B_2O_3$ molecules. The $B_2O_3$ activity was obtained by the ion currents comparison method and the SrO activity was calculated according to the Gibbs–Duhem equation. The resulting Gibbs energy function of formation demonstrated negative deviations from the ideal behaviour with maximal divergence at equimolar composition of oxides in the $SrO-B_2O_3$ system. From the obtained values of the Gibbs

**Table 6**. Enthalpies of formation of crystalline strontium borates from elements ($\Delta H^\circ_{f,298}$) and from the constituent oxides ($\Delta H^\circ_{f,ox,298}$).[79]

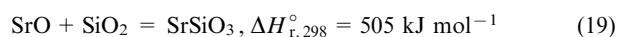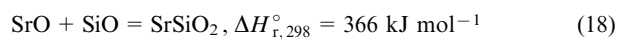| Compound | $-\Delta H^\circ_{f,298}$, kJ mol$^{-1}$ | $-\Delta H^\circ_{f,ox,298}$, kJ mol$^{-1}$ |
|---|---|---|
| $SrO \cdot 2\,B_2O_3$ | 3181 | 43.5 |
| $SrB_2O_4$ | 1902 | 37.6 |
| $2\,SrO \cdot B_2O_3$ | 2489 | 34.5 |

energy of formation, the enthalpy of formation of strontium borates was derived, as presented in Table 6.

### 4.2. The $SrO-SiO_2$ system

Since the vapour composition depended greatly on interaction of the samples under study with the container material, a number of additional peaks of mass spectra of vapour over the $SrO-SiO_2$ system had to be analyzed.[69, 81, 82]

As a first step, samples of this system containing from 10 up to 90 mol.% SrO were vapourized from a molybdenum effusion cell. In the temperature range of 1840 – 1970 K, SiO, SrO, Sr, $MoO_2$, $MoO_3$, $SrMoO_3$, $SrMoO_4$, and $O_2$ molecular species were identified in the vapour over these samples. The SrO and $SiO_2$ activities in $SrO-SiO_2$ glasses and melts were determined by differential mass spectrometry taking pure strontium and silicon oxides as reference substances. In the range of compositions 20 – 67 mol.% of SrO, these results were verified by calculations of the SrO and $SiO_2$ activities using the Belton–Fruechan and Gibbs–Duhem equations. The Gibbs energy of formation drawn from the component activity data indicated negative deviations from ideal behaviour in the $SrO-SiO_2$ system.

Since ions of gaseous strontium silicates had the same $m/z^+$ value as the molybdenum-containing vapour species, tungsten effusion cells had to be used to facilitate their detection. Gaseous strontium silicates had to be vapourized from a tungsten effusion cell to facilitate deciphering of their mass spectra of vapour. At the temperature range of 2180 – 2340 K in the vapour over a sample containing 66.7 mol.% of strontium oxide, the SrO, SiO and $SrSiO_2$ vapour species were identified in addition to other molecular forms. To determine the standard enthalpies of formation of gaseous strontium silicates, temperature dependences of the equilibrium constants of the gas-phase reactions were obtained:[69]

$$SrO + SiO = SrSiO_2, \ \Delta H^\circ_{r,298} = 366 \text{ kJ mol}^{-1} \quad (18)$$

$$SrO + SiO_2 = SrSiO_3, \ \Delta H^\circ_{r,298} = 505 \text{ kJ mol}^{-1} \quad (19)$$

By combining the enthalpies of reactions with the enthalpies of formation of the SrO, SiO, and $SiO_2$ vapour species, the standard enthalpies of formation and atomization were calculated:[69]

| | $\Delta H^\circ_{f,298}$, kJ mol$^{-1}$ | $\Delta H^\circ_{at,298}$, kJ mol$^{-1}$ |
|---|---|---|
| $SrSiO_2$ | $-474$ | 1583 |
| $SrSiO_3$ | $-841$ | 2199 |

### 4.3. The $SrO-B_2O_3-SiO_2$ system

The efficiency of immobilization of radioactive components incorporated into glass matrixes depends first of all on their components thermodynamic activities. The activity of high-level radioactive strontium oxide in borosilicate glasses widely used for these purposes was studied recently[83] in a wide concentration range of the $SrO-B_2O_3-SiO_2$ system.

12 of 22

V.L.Stolyarova, A.L.Shilov, T.V.Sokolova, M.Kurata, D.Costa
*Russ. Chem. Rev.*, 2023, **92** (5) RCR5059

The samples containing $10-60$ mol.% SrO were vapourized from molybdenum effusion cell in the temperature range of $1700-1800$ K and since their melting points did not exceed 1600 K, all of them were supposed to be in the molten state. Mass spectra of the vapour over these melts illustrated that $B_2O_3$, SiO, $SrB_2O_4$ and molybdenum oxides were the main vapour species over $SrO-B_2O_3-SiO_2$ melts.

The SrO, $B_2O_3$ and $SiO_2$ activities were calculated at the temperatures of 1720 and 1800 K by integration of the ratios of the measured ion currents in mass spectra of vapour over the $SrO-B_2O_3-SiO_2$ system, which required employing the earlier obtained data on the $B_2O_3$ and $SiO_2$ activities in the corresponding binary systems. The results were presented in the form of the SrO, $B_2O_3$ and $SiO_2$ isoactivity contours and curves of constant values of excess Gibbs energy in the composition triangles of the $SrO-B_2O_3-SiO_2$ system. $SrO-B_2O_3-SiO_2$ melts exhibited negative deviations from the ideal behaviour, which could be related to the strong chemical interactions between components in condensed phase with the formation of compounds. The component activity coefficients decreased from 0.2 for the samples with high SrO concentration to 0.0002 for the samples with minimal concentration and at higher temperature the deviations increased.

### 4.4. The $SrO-MoO_3$ system

The gaseous strontium molybdates were studied by vapourization from molybdenum effusion cells at the temperature range of $1947-2085$ K.[84] To increase the relative contents of strontium molybdates in the vapour, samples were loaded into the cell in the form of strontium oxide mixed with $MoO_2$, which disproportionated on heating into Mo and $MoO_3$.

The partial pressures of the vapour species measured by the ion currents comparison method were used to calculate the equilibrium constants of gas-phase reactions

$$SrO + MoO_3 = SrMoO_4 \qquad (20)$$

$$SrO + MoO_2 = SrMoO_3 \qquad (21)$$

The average values of the enthalpies of reactions (20) and (21) were obtained as 532.6 and 546.0 kJ mol$^{-1}$, respectively. With additional reference data for enthalpies of formation of the SrO, $MoO_2$, and $MoO_3$ vapour species, the standard enthalpies of formation and atomization of strontium molybdates were calculated. Thermodynamic data for strontium molybdates are presented in Table 7.

Kazenas *et al.*[85] investigated strontium molybdate sublimation using standard KEMS techniques at significantly lower temperatures. Solid samples of $SrMoO_4$ were vapourized from platinum effusion cells in the temperature range of $1570-1800$ K. Mass spectrum of the vapour over $SrMoO_4$ revealed that the gaseous phase was formed mainly

**Table 7.** Standard enthalpies of formation and atomization as well as entropies of the gaseous strontium and barium molybdates and molybdites.[84]

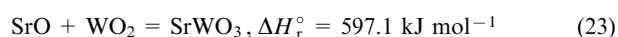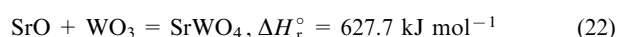| Gaseous species | $-\Delta H^{\circ}_{f,298}$, kJ mol$^{-1}$ | $\Delta H^{\circ}_{at,298}$, kJ mol$^{-1}$ | $S^{\circ}_{298}$, J (mol K)$^{-1}$ |
|---|---|---|---|
| $SrMoO_4$ | $912 \pm 4$ | $2727 \pm 6$ | 367.3 |
| $SrMoO_3$ | $577 \pm 3$ | $2143 \pm 6$ | 346.3 |
| $BaMoO_4$ | $985 \pm 11$ | $2818 \pm 13$ | 377.2 |
| $BaMoO_3$ | $647 \pm 13$ | $2231 \pm 15$ | 356.4 |

by the $SrMoO_4$ gaseous species with negligible admixture of atomic strontium. Thus, according to Ref. 85 strontium molybdate sublimed congruently, without dissociation.

Standard enthalpies of sublimation $\Delta H^{\circ}_{s,0}(SrMoO_4)$ determined by the 2nd and 3rd law treatment were 500 and 482 kJ mol$^{-1}$, respectively. The atomization energy of the $SrMoO_4$ gaseous molecule calculated in Ref. 85, $\Delta H^{\circ}_{at,0} = 2860$ kJ mol$^{-1}$, was found to be comparable with the results obtained in Ref. 84 (see Table 7).

### 4.5. $SrWO_4$

Gaseous alkaline earth tungstates were studied in Ref. 84 using the same experimental techniques as those for strontium molybdates described above. To provide $SrWO_3$ partial pressure in vapour sufficiently high for measuring equilibrium constant, a double two-temperature effusion cell was used. In the high-temperature compartment with effusion orifice, strontium oxide was placed. The lower temperature compartment connected to the first one by a canal in the crucible was charged with $WO_2$ and $HWO_4$ providing coexistence of SrO and $WO_2$ in the vapour.

In the temperature range of $2232-2408$ K, the SrO, $SrWO_3$, $SrWO_4$ and tungsten oxide vapour species were detected in the gaseous phase of this mixture. From the measured values of partial pressures of these vapour species, average enthalpies of the following gaseous reactions were calculated:

$$SrO + WO_3 = SrWO_4, \Delta H^{\circ}_r = 627.7 \text{ kJ mol}^{-1} \qquad (22)$$

$$SrO + WO_2 = SrWO_3, \Delta H^{\circ}_r = 597.1 \text{ kJ mol}^{-1} \qquad (23)$$

Thermodynamic data obtained in Ref. 84 for the gaseous strontium tungstates are summarized in Table 8.

Pre-synthesized samples of solid $SrWO_4$ were studied by Kazenas *et al.*[86] These samples were vapourized from platinum effusion cells at the temperature range of $1805-1890$ K. Deciphering of the mass spectrum of the vapour over $SrWO_4$ indicated that strontium tungstate evapourated without dissociation in the form of the gaseous $SrWO_4$. Standard enthalpies of sublimation $\Delta H^{\circ}_{s,0}(SrWO_4)$ determined by the 2nd and 3rd law treatment were 610 and 620 kJ mol$^{-1}$, respectively. The calculated atomization energy of the gaseous $SrWO_4$ molecule, $\Delta H^{\circ}_{at,0}(SrWO_4) = 3060$ kJ mol$^{-1}$, was in reasonable agreement with the value obtained earlier in Ref. 84 (Table 8).
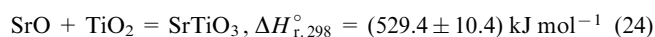
**Table 8.** Standard enthalpies of formation and atomization as well as entropies of the gaseous strontium- and barium tungstates and tungstites.[84]

| Gaseous species | $-\Delta H^{\circ}_{f,298}$, kJ mol$^{-1}$ | $\Delta H^{\circ}_{at,298}$, kJ mol$^{-1}$ | $S^{\circ}_{298}$, J (mol K)$^{-1}$ |
|---|---|---|---|
| $SrWO_4$ | $962 \pm 9$ | $2971 \pm 11$ | 371.9 |
| $SrWO_3$ | $583 \pm 4$ | $2343 \pm 7$ | 351.4 |
| $BaWO_4$ | $1025 \pm 13$ | $3052 \pm 15$ | 381.6 |
| $BaWO_3$ | $658 \pm 13$ | $2437 \pm 15$ | 361.3 |

### 4.6. The $SrO-TiO_2$ system

The samples of the $SrO-TiO_2$ system were prepared by thermal decomposition of a mixture of $TiO_2$ and $SrCO_3$ taken in a 1:1 molar ratio directly in the tungsten effusion cell and then vapourized in the temperature range of $2100-2400$ K.[87] The main vapour species identified in the gaseous phase were SrO, TiO, $TiO_2$ and $SrTiO_3$. Their

V.L.Stolyarova, A.L.Shilov, T.V.Sokolova, M.Kurata, D.Costa
*Russ. Chem. Rev.*, 2023, **92** (5) RCR5059

13 of 22

partial pressures of vapour species were used for the calculation of the equilibrium constant of gaseous reaction

$$SrO + TiO_2 = SrTiO_3, \Delta H^\circ_{r, 298} = (529.4 \pm 10.4) \text{ kJ mol}^{-1} \quad (24)$$

in the narrow temperature range (2353 – 2365 K) insufficient for derivation of its temperature dependence. The $SrTiO_3$ standard enthalpies of formation ($\Delta H^\circ_{f, 298} = -868$ kJ mol$^{-1}$) and atomization ($\Delta H^\circ_{at, 298} = 2249$ kJ mol$^{-1}$) were calculated.

In the HTMS study by Rangel-Salinas *et al.*,[88] the SrO activity in the $SrO-TiO_2$ system was measured as a function of composition to clarify the observed discrepancy between the phase diagrams and the thermodynamic data available in the temperature range of 1853 – 1973 K. A distinctive feature of the experimental setup was abnormally massive samples and, accordingly, large dimensions of the crucible: quadruple $Pt-20\%$ Rh effusion cell with orifices 2 mm in diameter was charged with 1 g of a reference substance as SrO and three samples of the $SrO-TiO_2$ system, 1 g each, having different content of SrO and $SrTiO_3$ components. In the vapour over the $SrO-TiO_2$ system Sr, SrO, O and $O_2$ molecular species were detected. In the end of vapourization runs the samples were quenched for XRD analysis and mass-loss measurements. The results confirmed the existence of the $Sr_2TiO_4$, $Sr_3Ti_2O_7$ and $SrTiO_3$ phases and did not support the data predicting the existence of $Sr_2TiO_4$, $Sr_4Ti_3O_{10}$ and $SrTiO_3$ phases in the examined concentration range.

### 4.7. The SrO − Nb₂O₅ system

The samples of the $SrO-Nb_2O_5$ system prepared by decomposition of a mixture of $Nb_2O_5$ and $SrCO_3$ taken in an equimolar ratio were vapourized from a tungsten effusion twin cell.[89] Analysis of the recorded mass spectrum of the vapour over this mixture led to a conclusion that $SrNbO_2$, $SrNbO_3$ and $SrNb_2O_6$ were the molecular precursors of the detected ions in mass spectra of vapour over this mixture.

The partial pressures of the $SrNbO_2$, $SrNbO_3$, and $SrNb_2O_6$ vapour species were measured by differential mass spectrometry using standard approaches. From the obtained experimental values of partial pressures of these vapour species, the thermodynamic functions of strontium niobate were deduced (Table 9).

### 4.8. SrCoO₂

To explore the gaseous $SrCoO_2$ molecule, the mixtures of $Co_3O_4$ and SrO were vapourized from molybdenum twincells in the temperature range of 1691 – 2097 K.[90] The mass

**Table 9.** Enthalpies of the gaseous reactions and standard enthalpies of formation as well as atomization of gaseous strontium- and barium niobates.[89]

| Reaction | $\Delta H^\circ_{r, 298}$, kJ mol$^{-1}$ | $-\Delta H^\circ_{f, 298}$, kJ mol$^{-1}$ | $\Delta H^\circ_{at, 298}$, kJ mol$^{-1}$ |
|---|---|---|---|
| $SrO + NbO_2 = SrNbO_2$ | $526 \pm 3$ | $741 \pm 3$ | $2372 \pm 6$ |
| $BaO + NbO_2 = BaNbO_3$ | $455 \pm 20$ | $784 \pm 20$ | $2434 \pm 21$ |
| $Ba + NbO_2 = BaNbO_2$ | $284 \pm 9$ | $303 \pm 10$ | $1704 \pm 12$ |
| $BaO + NbO = BaNbO_2$ | $388 \pm 6$ | $305 \pm 7$ | $1706 \pm 10$ |
| $BaO + 3 NbO_2 =$ $= BaNbO_2O_6 + NbO$ | $935 \pm 26$ | $1877 \pm 27$ | $4997 \pm 30$ |
| $2 BaO + 2 NbO_2 =$ $= BaNb_2O_6 + Ba$ | $1031 \pm 29$ | $1868 \pm 30$ | $5006 \pm 32$ |
| $2 BaNbO_3 + NbO_2 =$ $= BaNb_2O_6 + NbO + BaO$ | $11 \pm 19$ | $1864 \pm 20$ | $5002 \pm 27$ |

spectrum analysis of vapour over this mixture indicated that the gaseous phase was composed of the Sr, SrO, Co, CoO, $SrCoO_2$ vapour species and the species formed by interaction of a sample with molybdenum walls of the cell.

Evaluation of the thermodynamic functions of the gaseous $SrCoO_2$ species was based on the measured partial pressures of the corresponding vapour species and equilibrium constant of the gaseous reaction:

$$SrO + CoO = SrCoO_2 \quad (25)$$

Using standard approaches, the values of enthalpy of formation ($\Delta H^\circ_{f, 298} = -149$ kJ mol$^{-1}$) and atomization ($\Delta H^\circ_{at, 298} = 1233$ kJ mol$^{-1}$) of the gaseous $SrCoO_2$ molecule were found.

### 4.9. The SrO − BeO system

Beryllium oxide is known to form oligomers $(BeO)_n$ in the vapour that may exhibit basic or acidic properties depending on the experimental conditions. Thus, in the gaseous salts, BeO may be both cation- and anion-forming oxide. These two cases were studied by HTMS of strontium berillates.[91] To vapourize the SrO and BeO mixture, a uniform temperature tungsten effusion cell was employed. In the temperature range of 2140 – 2425 K, the Sr, SrO, $SrBeO_2$ and $Be_nO_n$ vapour species were identified. To find standard enthalpies of formation of the gaseous $SrBeO_2$ molecule, the equilibrium constants and enthalpies of the following gaseous reactions were determined using the measured partial pressures of the corresponding vapour species:

$$SrO + 1/3 Be_3O_3 = SrBeO_2 \quad (26)$$
$$SrO + 1/4 Be_4O_4 = SrBeO_2 \quad (27)$$

The results of calculations of the thermodynamic functions for the gaseous $SrBeO_2$ molecule are presented in Table 10 in comparison with the results for barium beryllates.

**Table 10.** Enthalpies and standard entropies of reaction as well as enthalpies of formation and atomization of the gaseous strontium- and barium berrilates.[91]

| Vapour species | Temperature range, K | $-\Delta H^\circ_{r, 0}$, kJ mol$^{-1}$ | $-\Delta H^\circ_{f, 298}$, kJ mol$^{-1}$ | $\Delta H^\circ_{at, 298}$, kJ mol$^{-1}$ | $\Delta S^\circ_{298}$, J (mol K)$^{-1}$ |
|---|---|---|---|---|---|
| $SrBeO_2$ | 2138 – 2424 | $81 \pm 3$ | $436 \pm 24$ | $1419 \pm 25$ | 323.1 |
| $BaBeO_2$ | 2154 – 2298 | $17 \pm 4$ | $485 \pm 21$ | $1486 \pm 22$ | 337.2 |

### 4.10. The SrO − Al₂O₃ system

The thermodynamic properties of the $SrO-Al_2O_3$ system were studied by KEMS and were fitted by the Redlich−Kister and Wilson polynomials.[92, 93] Samples under study were obtained by solid-state synthesis and identified by X-ray fluorescence analysis, X-ray phase analysis, scanning electron microscopy, electron probe microanalysis, simultaneous thermal analysis, and thermogravimetric analysis. The thermodynamic values obtained were also optimized using the GLTAS approach. The vapour composition, temperature, and concentration dependences of the partial vapour pressures over the samples under study as well as the SrO activities in melts of the $SrO-Al_2O_3$ system were determined by the KEMS method. Usage of the Redlich−Kister and Wilson polynomials allowed calculation of the excess Gibbs energies, enthalpies of mixing, and excess entropies in the concentration range
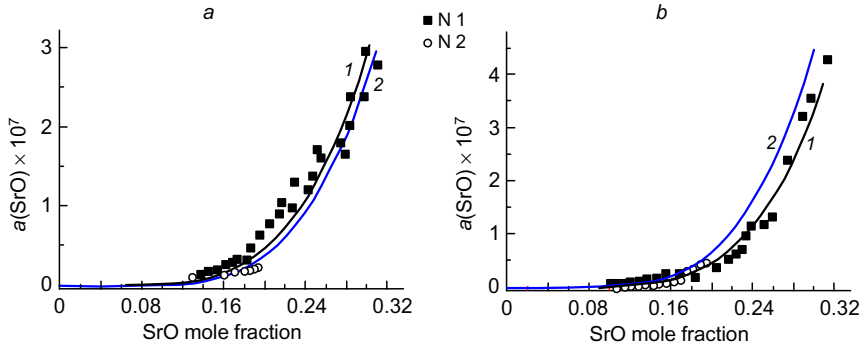
**Figure 9.** The SrO activities, $a$(SrO), in the melts of the $SrO-Al_2O_3$ system obtained as a result of complete vapourization of sample N 1 and sample N 2 at temperatures of 2450 (*a*) and 2550 K (*b*). *1* and *2* are the approximations of the SrO activity values using the Redlich–Kister polynomial and Wilson polynomial, respectively.[92, 93]
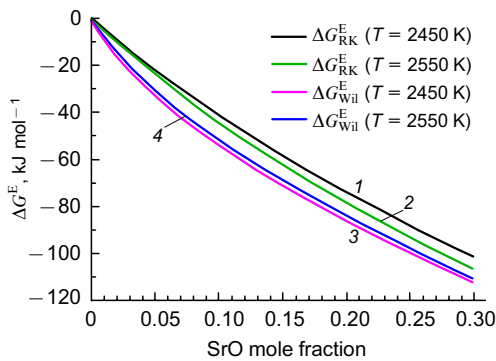


**Figure 10.** The excess Gibbs energy values in the melts of the $SrO-Al_2O_3$ system using the Redlich–Kister polynomial $\Delta G_{RK}^E$ — *1* and *2*, and Wilson polynomial $\Delta G_{Wil}^E$ — *3* and *4*, at temperatures of 2450 (*1*, *3*) and 2550 K (*2*, *4*).[92, 93]

$0-33$ mol.% of SrO at the temperatures of 2450 and 2550 K, Figs 9–12. Significant negative deviations from the ideality were observed in the melts of the $SrO-Al_2O_3$ system at the temperatures 2450, 2550, and 2650 K. The

Wilson polynomial was found to be the optimal approach to describe the thermodynamic properties in the system studied. Optimization of the experimental data using the GLTAS approach allowed the characteristic features of the thermodynamic description of the $SrO-Al_2O_3$ system to be elucidated and explained.
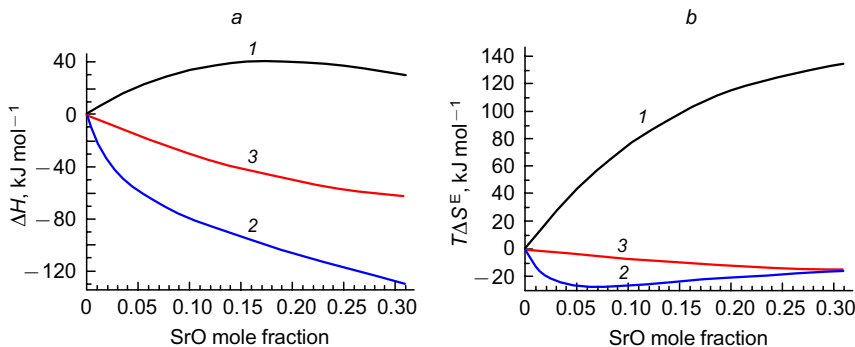
The concentration dependence of the excess Gibbs energy in the $SrO-Al_2O_3$ system was described using the Wilson polynomial as:[93]

$$\Delta G^E = RT(-x_{SrO}\ln(x_{SrO} + \Lambda_{SA}x_{Al_2O_3}) - \qquad (28)$$
$$- x_{Al_2O_3}\ln(\Lambda_{AS}x_{SrO} + x_{Al_2O_3}))$$

where $x_{SrO}$ and $x_{Al_2O_3}$ are mole fractions of strontium and aluminium oxides, respectively, and $\Lambda_{SA}$, $\Lambda_{AS}$ are parameters of the Wilson equation.

### 4.11. The $La-Sr-Ca-Cr-O$ system

Peck *et al.*[94] investigated perovskite phases of the composition $La_{0.80}Sr_{0.2-x}Ca_xCrO_{3-\delta}$ by the KEMS method. Three samples ($x = 0.05$, 0.10 and 0.15) were prepared from nitrates mixtures. For vapourization, tungsten effusion cells coated with iridium were used. Composition of the



**Figure 11.** The enthalpies of mixing ($\Delta H$) — (*a*) and excess entropies multiplied by temperature ($T\Delta S^E$) — (*b*) in the melts of the $SrO-Al_2O_3$ system at a temperature of 2450 K: *1*, calculated by the Redlich–Kister polynomials; *2*, calculated by the Wilson polynomials; and *3*, accepted from the NUCLEA database.[93]
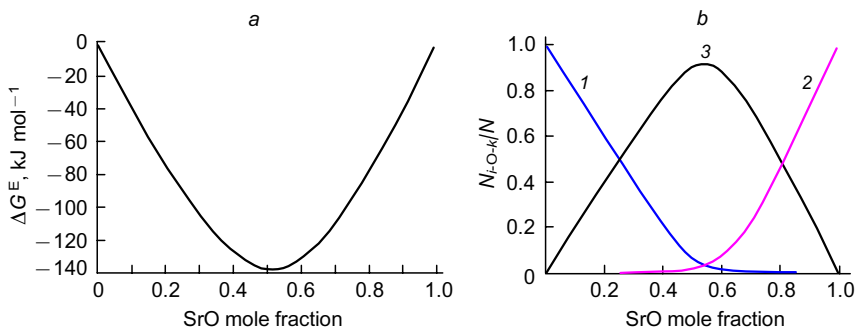


**Figure 12.** The results of the optimization of the SrO activities in the melts of the $SrO-Al_2O_3$ system at 2550 K within the GLTAS approach: (*a*), the concentration dependence of the excess Gibbs energies ($\Delta G^E$, in kJ mol$^{-1}$); and (*b*), the relative amounts $N_{i\text{-}O\text{-}k}/N$ of the bonds of different types: *1* is $Al-O[Al]$, *2* is $Sr-O[Sr]$, *3* is $Sr-O[Al]$ where the atoms in brackets correspond to the second coordination sphere.[93] $N_{i\text{-}O\text{-}k}$ denotes the number of contacts between *i*- and *k*-type contact points and $N$ — the total number of contacts in GLTAS model.

V.L.Stolyarova, A.L.Shilov, T.V.Sokolova, M.Kurata, D.Costa
*Russ. Chem. Rev.*, 2023, **92** (5) RCR5059

15 of 22

gaseous phase determined over the samples at a temperature of 2000 K was rather complicated and contained the Cr, CrO, $CrO_2$, CaO, Sr, SrO and LaO vapour species. The thermodynamic component activities were found from the partial pressures of vapour species over the samples under study and over pure $Cr_2O_3$, SrO, and CaO. The $La_2O_3$ activity in the $La-Sr-Ca-Cr-O$ system was determined using earlier obtained data. Two principal conclusions were made in the study:[94] (i) the perovskite $La_{1-x}M_xCrO_{3-\delta}$ phase remains stable on doping by M atoms under low oxygen pressure at 1873 K up to $x = 0.31$ for Sr; (ii) it is possible to replace Sr by Ca on the La perovskite sublattice at least up to 15 mol.%.

# 5. The Ba-bearing systems

Study of the vapourization processes of the oxide systems containing barium and strontium were often carried out concurrently since both SrO and BaO were considered previously in view of their application in vacuum electronics as materials for electron emitters and residual gas absorbers. Some references mentioned in previous Section IV included studies of the systems containing barium oxide also because together with strontium oxide it is a radioactive product in the waste of nuclear power plants.

## 5.1. The $BaO-B_2O_3$ system
High temperature behaviour of the $BaO-B_2O_3$ system was studied using the KEMS method for $3\,BaO\cdot B_2O_3$, $BaO\cdot B_2O_3$, $BaO\cdot 2\,B_2O_3$ by Asano and Kou[75-78] as well as for the samples containing 20, 30 and 37 mol.% BaO by Stolyarova and co-workers.[95,96] In comparison with the content of vapour identified over $BaO\cdot 2\,B_2O_3$ in Ref. 78 see Table 4), Refs 95, 96 showed that $B_2O_3$ and $Ba(BO_2)_2$ were the main vapour species over this system in the temperature range of $1473-1523$ K. It may be one of the reasons why enthalpy of formation of $Ba_3B_2O_6$ found by Cordfunke et al.[97] using the drop calorimetry method was very different from the value derived by Asano and Kou[78] (see Table 5). The $B_2O_3$ and $Ba(BO_2)_2$ activities obtained in the $BaO-B_2O_3$ system illustrated the negative deviations from the ideality at the temperature of 1473 K.[95,96]

Barium borates were studied to get a deeper insight into the laws of association of oxide species in the vapour and to corroborate the findings published earlier.[98] The samples containing $BaB_2O_4$ and $2\,BaO\cdot B_2O_3$ were vapourized from platinum and molybdenum Knudsen cells. Ionic species in the recorded mass spectra of vapour over these compounds in the temperature range of $1600-1650$ K were identical for both compositions.

The temperature dependence of mass spectra of vapour over $BaB_2O_4$ and $2\,BaO\cdot B_2O_3$ in the temperature range between 1600 and 2000 K could be explained by assuming that the content of the gaseous phase in the effusion cell depended on the balance of two coexisting processes such as vapourization and thermal dissociation reactions:

$$BaB_2O_4(l) = BaB_2O_4(g) \tag{29}$$

$$BaB_2O_4(l) = BaO(s) + B_2O_3(g) \tag{30}$$
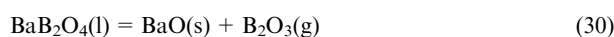
The equilibrium (29) strongly depends on temperature. Enthalpy of this reaction obtained from the temperature dependence of the ion currents in mass spectra of vapour over $BaB_2O_4$ was used to evaluate the standard enthalpies of formation and atomization and gave the values of

$\Delta H^{\circ}_{f,0}(BaB_2O_4\,,s) = (-1424\pm 28)$ kJ mol$^{-1}$ and $\Delta H^{\circ}_{at,0}(BaB_2O_4\,,s) = (3730\pm 28)$ kJ mol$^{-1}$.

Vapourization of the sample containing $2\,BaO\cdot B_2O_3$ at the temperature of 1900 K allowed to determine the thermodynamic properties of the gaseous $BaBO_2$ molecule such as $\Delta H^{\circ}_{f,0} = (-598\pm 15)$ kJ mol$^{-1}$ and $\Delta H^{\circ}_{at,0} = (1850\pm 16)$ kJ mol$^{-1}$ from the equilibrium constant of the following reaction:

$$BaBO_2(g) = Ba(g) + BO_2(g) \tag{31}$$

Further, the $BaO-B_2O_3$ system was studied in a wide range of compositions when the samples containing 0.1, 0.2, 0.3, 0.33, 0.4, 0.5, 0.6, 0.67, 0.75 mole fractions of BaO were vapourized from molybdenum cells at the temperature range of $1500-1650$ K.[80] It should be mentioned that in this temperature range the melts area on the phase diagram extends from 5 to 100 mol.% of $B_2O_3$.

The $B_2O_3$ activities were determined from the measured ion currents of the gaseous species in mass spectra of vapour over the $BaO-B_2O_3$ system by two mainly independent methods. The BaO activity calculated by the Gibbs–Duhem equation allowed obtaining the Gibbs energy in the melts of the $BaO-B_2O_3$ system. It was shown that the melts were characterized by the negative deviations from the ideal behaviour, which may result from formation of stable chemical compounds in the condensed phase in the system under consideration. Maximal deviation was observed at the equimolar ratio of the BaO and $B_2O_3$.

## 5.2. The $BaO-SiO_2$ system
The data on the vapourization behaviour of barium silicate is required in the nuclear plants safety analysis since it may be formed during severe accidents by core-concrete interactions. According to the high temperature mass spectrometric study of vapour over $BaSiO_3$, Cordfunke et al.[99] discovered the existence of the gaseous barium silicate molecule $BaSiO_3$ and discussed its thermodynamic stability. Greater part of the work was devoted to the calculations of the structure of the $BaSiO_3$ vapour molecule that could be accepted for the subsequent thermodynamic calculations. Three hypothetic structures were considered and the most probable was found to be the configuration with two bridging oxygen atoms between barium and silicon atoms.

The $BaSiO_3$ sample was vapourized in the temperature range of $1783-2143$ K from tungsten effusion cells. The vapour consisted of the Ba, BaO, SiO, $SiO_2$ and $BaSiO_3$ gaseous species. From the measured temperature dependence of the $BaSiO_3^+$ ion current in mass spectra of vapour over $BaSiO_3$, the enthalpy of reaction

$$BaSiO_3(s) = BaSiO_3(g) \tag{32}$$

was obtained according to the 2nd law of thermodynamics for the further evaluation of the enthalpy of sublimation, $\Delta H^{\circ}_{s,298} = (560.6\pm 21.3)$ kJ mol$^{-1}$. The data of Ref. 99 was treated once more in Ref. 100 to obtain the standard enthalpy of formation of barium silicate $\Delta H^{\circ}_{f,298} = (-1045.8\pm 21.3)$ kJ mol$^{-1}$. It was also found that the concentration of the BaO gaseous species in the vapour over $BaSiO_3$ was relatively small, so the main species of the vapour were the gaseous $BaSiO_3$ molecules.[99]

According to Refs 100, 101, the entirely different results were obtained on the vapourization processes in the $BaO-SiO_2$ system in the temperature range of $2132-2263$ K. Mixtures of $BaCO_3$ and $SiO_2$ of various compositions were loaded into molybdenum twin effusion

16 of 22

V.L.Stolyarova, A.L.Shilov, T.V.Sokolova, M.Kurata, D.Costa
*Russ. Chem. Rev.*, 2023, **92** (5) RCR5059

cells, calcined at the temperature 1670 K and then evapourated. The partial pressures of vapour species were determined by differential mass spectrometry techniques and the derivation of thermochemical properties was based on quantum chemical calculations.

Since volatility of BaO was higher than that of $SiO_2$, the samples became enriched with silicon oxide during the experimental runs. Due to the intense interaction of the vapour with the material of container, considerable amounts of molybdenum oxides and barium molybdates were presented in the vapour over samples in the $BaO-SiO_2$ system.

Thus, it was demonstrated that the vapour over the $BaO-SiO_2$ system was composed of the Ba, BaO, SiO, $SiO_2$, $BaSiO_2$ and $BaSiO_3$ species and the vapourization process was not congruent. After measuring the partial pressures of the corresponding vapour species, the following two gas-phase reactions were considered

$$BaO + SiO = BaSiO_2 \qquad (33)$$

$$BaO + SiO_2 = BaSiO_3 \qquad (34)$$

in order to calculate the 3rd law enthalpies of reactions (33) and (34). The resulting standard formation enthalpies for gaseous $BaSiO_2$ and $BaSiO_3$ were $\Delta H^{\circ}_{f,298} = (-510 \pm 15)$ and $(-884 \pm 18)$ kJ mol$^{-1}$, respectively, and the resulting standard atomization enthalpies for $BaSiO_2$ and $BaSiO_3$ corresponding to the reactions

$$BaSiO_n(g) = Ba(g) + Si(g) + nO(g) \qquad (35)$$
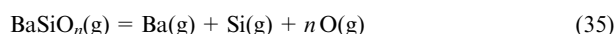
($n = 2, 3$) were $\Delta H^{\circ}_{at,298}(BaSiO_2) = (1637 \pm 17)$ kJ mol$^{-1}$ and $\Delta H^{\circ}_{at,298}(BaSiO_3) = (2261 \pm 20)$ kJ mol$^{-1}$.

In contrast to Ref. 99, the dissociative vapourization was found to be the prevailing process in the $BaO-SiO_2$ system. One of the main vapour species was BaO, whereas $BaSiO_2$ and $BaSiO_3$ partial pressures were less than 0.1% of the total vapour pressure. That could be one of the reasons for the difference in the $\Delta H^{\circ}_{f,298}(BaSiO_3)$ gaseous molecule values exceeding 200 kJ mol$^{-1}$ reported in Ref. 99, 100.

It should be mentioned that the obtained thermodynamic values clearly demonstrate the validity of one of the acid-base approaches [8, 87] to the problem of stability of gaseous salts proposed in earlier studies. For the isocation series of gaseous oxyacid salts, a linear relationship was suggested between the atomization enthalpy of $M_mXO_n$ and the atomization enthalpy of corresponding anion-forming oxides $XO_n$:

$$\Delta H^{\circ}_{at,298}(M_mXO_n, gas) = k\,\Delta H^{\circ}_{at,298}(XO_n, gas) + b \qquad (36)$$

where X is the anion-forming element and $k$ and $b$ are the adjustable parameters of the equation.

The values for $BaSiO_2$ and $BaSiO_3$ (for which $k = 1.035$ and $b = 950$) obtained in Ref. 87 fitted in well the general trend. It confirms that relationship (36) allows enthalpies of gaseous barium salts to be estimated and provides a method for checking the accuracy of the measured data.

The glass and glass-ceramics samples of the $BaO-SiO_2$ system prepared in advance were vapourized from the molybdenum effusion cells for obtaining thermodynamic properties of this system such as the component activities.[102] The partial pressures of vapour species over the $BaO-SiO_2$ system were found using the differential mass spectrometric technique. It was shown that at the stage of the initial temperature elevation up to 1970 K the vapour consisted of the SiO, BaO and oxygen gaseous species. At higher temperatures, $MoO_2$, $MoO_3$, $BaMoO_3$, and

$BaMoO_4$ appeared in the vapour phase due to interaction processes with the cell material.

The BaO activity was measured as the ratio of ion currents of the corresponding vapour species in mass spectra of the gaseous phase over the $BaO-SiO_2$ system and over pure BaO. The $SiO_2$ activity was determined experimentally and calculated using the Belton-Fruehan and the Gibbs-Duhem equations. All results were mutually consistent and could be used for the further modelling the thermodynamic properties of the $BaO-SiO_2$ system on the basis of GLTAS. Negative deviations from the ideality were observed, that were presumably caused by the formation of the $BaO \cdot 2SiO_2$, $2BaO \cdot 3SiO_2$, $BaO \cdot SiO_2$, and $2BaO \cdot SiO_2$ compounds in the condensed phase of the system under consideration.

## 5.3. The $BaO-B_2O_3-SiO_2$ system

Using high-temperature mass spectrometry, the thermodynamic properties of the melts in the $BaO-B_2O_3-SiO_2$ system were determined.[103] In the melts of the investigated system, negative deviations from the ideal behaviour were observed at the temperatures 1650 and 1730 K.

## 5.4. The $BaPO_3$ and $BaPO_2$ vapour species

For the investigation of gaseous barium phosphates, special experimental conditions were created enabling coexistence of gaseous BaO, PO, and $PO_2$ in the vapour.[104] Molybdenum double effusion cell was used for the vapourization. Barium oxide was loaded into the upper compartment heated to high temperature; lower compartment kept at the temperature $300-700$ K less was charged with barium diphosphate. Thus, the vapour in the upper compartment equipped with effusion orifice consisted of BaO with small admixture of Ba and $O_2$ (a result of BaO evapouration) plus $PO_2$, PO and $O_2$ (an inlet flow from the lower compartment). Partial pressures of the molecular species identified in the vapour over this mixture were defined by the equilibrium constants of two gas-phase reactions:

$$BaO + PO_2 = BaPO_3 \qquad (37)$$

$$BaO + PO = BaPO_2 \qquad (38)$$

The thermodynamic properties of the gaseous barium phosphates obtained using the equilibrium constants of reactions (37) and (38) were evaluated from the measured partial pressures of vapour species (Table 11).

**Table 11.** Standard enthalpies of formation and atomization as well as entropies of the gaseous barium phosphates.[104]

| Barium phosphates | $-\Delta H^{\circ}_{f,298}$, kJ mol$^{-1}$ | $\Delta H^{\circ}_{at,298}$, kJ mol$^{-1}$ | $\Delta S^{\circ}_{298}$, J (mol K)$^{-1}$ |
|---|---|---|---|
| $BaPO_3$ | $823 \pm 4$ | $2066 \pm 15$ | 345 |
| $BaPO_2$ | $504 \pm 6$ | $1497 \pm 17$ | 334 |

## 5.5. The $BaO-MoO_3$ system

Molybdenum is formed in high yields in the nuclear fission of uranium and plutonium and also it is one of the important construction materials of nuclear reactors. Thus, the data on the volatility of its compounds is significant for analysis of contamination of the environment in severe accidents on nuclear power plants.
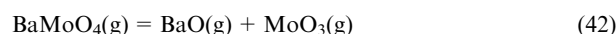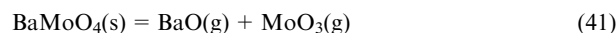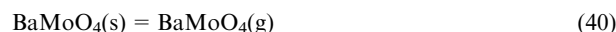
Kazenas *et al.*[105] investigated the $BaMoO_4$ sublimation at the temperature range of $1640-1770$ K by the standard HTMS techniques using molybdenum effusion cell. From

V.L.Stolyarova, A.L.Shilov, T.V.Sokolova, M.Kurata, D.Costa
*Russ. Chem. Rev.*, 2023, **92** (5) RCR5059

17 of 22

the mass spectrometric data and mass-loss measurements, the partial pressure of the $BaMoO_4$ vapour species was expressed as a function of temperature as

$$\log p(BaMoO_4, atm) = -17858/T + 4.38 \tag{39}$$

It was shown that the vapour over $BaMoO_4$ consisted of the gaseous $BaMoO_4$ molecules and lesser amounts of the $BaO$ and $MoO_3$ gaseous species. Evidence of the $Ba^+$ and $BaO^+$ ions presence in the mass spectra of vapour over $BaMoO_4$ was also found. Thus, vapourization process of barium molybdate was described in Ref. 105 by three reactions such as

$$BaMoO_4(s) = BaMoO_4(g) \tag{40}$$

$$BaMoO_4(s) = BaO(g) + MoO_3(g) \tag{41}$$

$$BaMoO_4(g) = BaO(g) + MoO_3(g) \tag{42}$$

On the basis of two sets of mass spectra recorded under the specified conditions, standard enthalpies of formation and atomization of $BaMoO_4$ and $BaMoO_3$ were determined (see Table 7).

### 5.6. BaWO$_4$

Vapourization of the liquid $BaWO_4$ sample was studied in Ref. 106. The samples were vapourized from tungsten effusion cells in the temperature range of $1770-1910$ K. The vapour composition over $BaWO_4$ was determined only tentatively. The mass-loss measurements indicated that the melt of $BaWO_4$ vapourized congruently with the formation of the $BaWO_4$ gaseous molecule partly dissociated to the $BaO$ and $WO_3$ gaseous species. By the least-squares approximation, the temperature dependence of the barium tungstate vapour partial pressure was obtained:

$$\log p(BaWO_4, atm) = -20570/T + 4.58 \tag{43}$$

From the measured partial vapour pressure of $BaWO_4$, the formation enthalpy, $\Delta H_{f,0}^{\circ} = (-1129 \pm 21)$ kJ mol$^{-1}$, and the atomization energy, $\Delta H_{at,0}^{\circ} = (3148 \pm 42)$ kJ mol$^{-1}$, of $BaWO_4(g)$ were calculated (see Table 8).

### 5.7. The BaO−Cr$_2$O$_3$ system

In the study,[107] the samples of the $BaO$-$Cr_2O_3$ system were vapourized from a tungsten effusion cell. The mass spectra of the vapour over the $BaO-Cr_2O_3$ system proved the presence of the $CrO$, $CrO_2$, $BaO$, $BaCrO_2$ and $BaCrO_3$ molecules, as well as chromium tungstates, oxygen, tungsten oxides, atomic chromium and barium gaseous species.

To determine the enthalpies of reactions involving gaseous barium chromates, the partial pressures of the species participating in gas-phase reactions were measured

$$BaO + CrO_2 = BaCrO_3 \tag{44}$$

$$BaO + CrO = BaCrO_2 \tag{45}$$
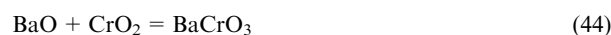
**Table 12.** Enthalpies of reactions (44) and (45), standard enthalpies of formation and atomization, as well as entropies of the gaseous barium chromate.[107]

| Reaction | $\Delta H_{r,298}^{\circ}$, kJ mol$^{-1}$ | $-\Delta H_{f,298}^{\circ}$, kJ mol$^{-1}$ | $\Delta H_{at,298}^{\circ}$, kJ mol$^{-1}$ | $\Delta S_{298}^{\circ}$, J (mol K)$^{-1}$ |
|---|---|---|---|---|
| (44) | $438.6 \pm 6.0$ | $674.8 \pm 8.0$ | $1985 \pm 19$ | 356.7 |
| (45) | $361.8 \pm 12.0$ | $304.5 \pm 12.1$ | $1382 \pm 24$ | 345.3 |

From the determined constants of the gas-phase equilibria (44) and (45), the values of the thermodynamic properties listed in Table 12 were derived.

### 5.8. BaTiO$_3$

The $BaTiO_3$ samples of special-purity grade were evaporated from tungsten effusion cells at temperatures of $2100-2400$ K.[87] The recorded mass-spectra of the vapour over $BaTiO_3$ and their dependence on the temperature suggested that the gaseous $Ba$, $BaO$, $TiO$, $TiO_2$ and $BaTiO_3$ species were available in the vapour over $BaTiO_3$.

The partial pressures of these species were measured by the ion current comparison method. For the gas-phase reaction

$$BaO + TiO_2 = BaTiO_3 \tag{46}$$

it was possible to measure the equilibrium constant as a function of temperature in a sufficiently wide temperature range of $2065-2300$ K. By the 2nd law treatment, the enthalpy of reaction (46) was calculated, $\Delta H_{r,298}^{\circ} = (435.8 \pm 5.0)$ kJ mol$^{-1}$. As a result, standard enthalpies of formation, $\Delta H_{f,298}^{\circ} = (-886.4 \pm 22.0)$ kJ mol$^{-1}$ and atomization, $\Delta H_{at,298}^{\circ} = (2286.4 \pm 32.1)$ kJ mol$^{-1}$, of $BaTiO_3$ needed for verification of the validity of equation (36) were computed.

### 5.9. The BaO−Fe$_3$O$_3$ system

The study[108] was aimed at the identification of barium ferrate molecule in the vapour. From comparison of reactivity of oxides in the vapour, a conclusion was made that gaseous $FeO$ should exhibit amphoteric properties and react with both anion- and cation-forming oxides to give gaseous salts. In barium ferrite, a iron oxide behaves as an anion-forming oxide.

Equimolar mixtures of $Fe_3O_4$ and $BaO$ were loaded into the tungsten effusion cell and evapourated in the temperature range of $1880-2058$ K. Deciphering of mass-spectra of the vapour over this mixture showed that it was composed of the following gaseous species: $Fe$, $Ba$, $FeO$, $BaO$ and $BaFeO_2$, where barium ferrate was a newly identified gaseous compound. Accordingly, the main process of the barium ferrate formation was the gas-phase reaction:

$$BaO + FeO = BaFeO_2 \tag{47}$$
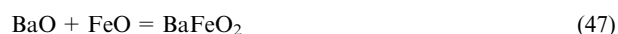
From the partial pressures of the vapour species measured over this mixture by the ion current comparison technique, the equilibrium constant of reaction (47) as a function of temperature was obtained. The enthalpy of reaction (47) was calculated by the 2nd and 3rd law treatment. The recommended standard enthalpy of formation of barium ferrate was $\Delta H_{f,298}^{\circ} = (-245.6 \pm 4.0)$ kJ mol$^{-1}$.[108]

### 5.10. The BaO−Co$_3$O$_4$ system

Vapourization of barium cobaltates was investigated using the traditional HTMS approach.[90] Mixtures of $Co_3O_4$ and $BaO$ were evapourated from molybdenum and tungsten effusion cells. In the temperature range of $1691-2097$ K, the vapour over these samples consisted of the $Ba$, $BaO$, $Co$, $CoO$ and $BaCoO_2$ molecular species with an admixture of gaseous products of $Mo$ and $W$ oxidation.

Temperature dependences of the partial pressures of the vapour species over these mixtures were determined and used to obtain the 3rd law enthalpies of the gas-phase reaction

$$BaO + CoO = BaCoO_2 \tag{48}$$

The data found were combined with the required quantum mechanical calculations to provide the following values of thermodynamic properties: $\Delta H^{\circ}_{\mathrm{f},298}(\mathrm{BaCoO_2}) = (-250 \pm 16)$ kJ mol$^{-1}$ and $\Delta H^{\circ}_{\mathrm{at},298}(\mathrm{BaCoO_2}) = (1353 \pm 20)$ kJ mol$^{-1}$.[90]

## 5.11. The BaO − BeO system

Beryllium oxide can exhibit amphoteric properties also as iron(II) oxide in the gaseous phase, being cation- or anion-forming oxide, and is liable to form polymeric gaseous species. Therefore, the formation of gaseous beryllates was anticipated in the high-temperature mass spectrometric study[91] of the BaO − BeO system vapourization.

Volatility of BaO and BeO is substantially different. Their coexistence in the gas-phase was provided by employing two-temperature double effusion cell made of molybdenum; barium oxide was loaded in the lower-temperature compartment and beryllium oxide — in the higher-temperature compartment of the cell. From the obtained mass spectral data describing gaseous phase over this mixture it was found that in the temperature range of 2150 – 2300 K the vapour consisted of the $\mathrm{Be}_n\mathrm{O}_n$ ($n = 1 – 5$), Ba, BaO and BaBeO$_2$ gaseous species.

Equilibrium constants of two following gas-phase reactions were deduced from the acquired experimental data:

$$\mathrm{BaO} + 1/3\,\mathrm{Be_3O_3} = \mathrm{BaBeO_2} \qquad (49)$$

$$\mathrm{BaO} + 1/4\,\mathrm{Be_4O_4} = \mathrm{BaBeO_2} \qquad (50)$$
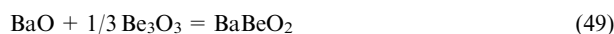
The thermodynamic values thus obtained were the averaged enthalpies of formation and atomization of the gaseous BaBeO$_2$ molecule ($\Delta H^{\circ}_{\mathrm{f},298} = (-485 \pm 21)$ kJ mol$^{-1}$ and $\Delta H^{\circ}_{\mathrm{at},298} = (1486 \pm 22)$ kJ mol$^{-1}$).

The thermodynamic data on gaseous beryllium salts confirmed that the linear dependence of atomization enthalpy of a salt on the atomization enthalpy of its oxide proposed earlier for the isocationic series of gaseous salts of oxygen-containing acids was also quite applicable to beryllium salts [see Eqn (36)].

## 5.12. The BaO − CeO$_2$ system

Vapourization processes and thermodynamic properties of CeO$_2$ and the BaO − CeO$_2$ system were studied in Ref. 109. The samples were vapourized from molybdenum and tungsten effusion cells. The partial pressures of vapour species were determined by the ion current comparison technique. Mass spectrum of the vapour over cerium dioxide recorded at the temperature range of 1906 – 2114 K indicated that the sample vapourized mainly in the form of the gaseous CeO$_2$ molecule. The temperature dependence obtained for the cerium dioxide partial pressure was expressed by equation

$$\log p(\mathrm{CeO_2, atm}) = -(28108 \pm 463)/T + 9.53 \pm 0.24 \qquad (51)$$

The BaO and CeO$_2$ mixture was examined in the temperature range of 1700 – 2100 K. Vapourization process of this mixture was not congruent; the condensed phase was enriched with cerium oxide in course of the experimental runs. The vapour over the samples of the BaO − CeO$_2$ system consisted of the Ba, BaO, CeO, CeO$_2$ and BaCeO$_3$ gaseous species. Their partial vapour pressures were used to calculate the equilibrium constant of the gas-phase reaction

$$\mathrm{BaO} + \mathrm{CeO_2} = \mathrm{BaCeO_3} \qquad (52)$$

on the basis of which the standard formation enthalpy of the gaseous BaCeO$_3$ molecule was determined as $\Delta H^{\circ}_{\mathrm{f},298} = (-1065 \pm 25)$ kJ mol$^{-1}$.

A substantial part of the study[109] was devoted to quantum chemical calculations of the gaseous compound formed according to the reaction (52). Two possible structures of the BaCeO$_3$ molecule were found to be equally energetically favorable and could be constituents of the vapour over the samples in the BaO − CeO$_2$ system.

## 6. Multicomponent oxide systems containing Cs-, Sr- and Ba-oxides

Despite advances in research on oxide systems using HTMS and its modification, KEMS, the number of multicomponent oxide systems containing Cs-, Sr- and Ba- oxides studied at present are extremely limited.

An original comparison of two methods of investigation of the vapourization processes of the experimental multicomponent glass containing, wt.%, SiO$_2$ — 53.8, Fe$_2$O$_3$ — 11.5, Al$_2$O$_3$ — 4.8, B$_2$O$_3$ — 6.5, Li$_2$O — 4.0, Na$_2$O — 8.6, MnO$_2$ — 3.6, NiO — 1.8, CaO — 1.0, MgO — 0.5, ZrO$_2$ — 3.8, SrO — 0.05, Cs$_2$O — 0.07, RuO$_2$ — 0.11 and Re$_2$O$_7$ — 0.03, that is the mass spectrometric Knudsen effusion method and the transpiration mass spectrometric method, was carried out by Hastie[110] in the temperature range of 973 – 1673 K. It was found out that lithium, sodium, and cesium metaborates are the main molecular species in the vapour over the glass under study and that the measured partial pressures of the alkaline metaborates in the temperature ranges common to both experimental methods are in reasonable mutual agreement.

The available data on the vapourization of Cs-bearing multicomponent oxide systems used for the incorporation of nuclear waste was also exemplary case analyzed in review.[111] The composition of the vapour phase over borosilicate glasses of various compositions studied by the high-temperature mass spectrometric method is listed in Table 13. It was also shown[111] that the CsBO$_2$ partial vapour pressures over these glasses may be presented as a function of the basicity of multicomponent oxide systems (defined as a ratio of the total concentration of alkali and alkali earth oxides to the total concentration of the acid

**Table 13**. The vapour composition over the borosilicate glasses used for the incorporation of nuclear waste at a temperature of 1270 K.[111]

| Glass No. | Content of oxides (wt.%) | | | | | | | | | Vapour species identified at $T = 1270$ K |
|---|---|---|---|---|---|---|---|---|---|---|
| | SiO$_2$ | Al$_2$O$_3$ | B$_2$O$_3$ | Na$_2$O | CaO | Li$_2$O | Cs$_2$O | Fe$_2$O$_3$ | others | |
| 1 | 45.5 | 4.9 | 14.0 | 9.9 | 4.0 | 2.0 | 1.4 | 2.9 | 15.4 | CsBO$_2$, NaBO$_2$, LiBO$_2$ |
| 2 | 45.3 | 4.9 | 14.0 | 9.8 | 4.0 | 2.0 | 1.4 | 2.9 | 15.7 | CsBO$_2$, NaBO$_2$, LiBO$_2$ |
| 3 | 46.6 | 5.0 | 14.2 | 10.0 | 3.0 | 3.0 | 0.8 | 2.0 | 15.4 | CsBO$_2$, NaBO$_2$, LiBO$_2$ |
| 4 | 46.2 | 4.2 | 13.4 | 9.1 | 2.5 | 3.4 | − | 5.2 | 16.0 | NaBO$_2$, LiBO$_2$, KBO$_2$ |
| 5 | 40.7 | 1.7 | 15.1 | 12.5 | 15.6 | − | 2.1 | 1.7 | 10.6 | CsBO$_2$, NaBO$_2$, KBO$_2$ |
| 6 | 43.0 | 2.8 | 20.5 | 16.4 | 11.6 | − | 1.8 | 3.9 | − | CsBO$_2$, NaBO$_2$, Na |

V.L.Stolyarova, A.L.Shilov, T.V.Sokolova, M.Kurata, D.Costa
*Russ. Chem. Rev.*, 2023, **92** (5) RCR5059

19 of 22

oxides in the melt or glass expressed in mole or weight percent).

# 7. Conclusion

The amount of the data on the vapourization behaviour of a wide variety of substances accumulated up to date makes possible the detailed analysis of the general features of the processes related to the formation of the vapour phase over oxide systems and the thermodynamic functions that can be derived from these data, especially for the systems containing $Cs_2O$, SrO and BaO. However, a lot of necessary information is still missing as can be seen from the review presented above. Therefore, a good deal of the recent HTMS studies were intended to fill these blank spaces, that is, to get information on the substances not yet examined, to identify a wider range of gaseous salts or oxides in different states of oxidation, to improve methods of evaluation of the thermodynamic functions that could be helpful in verification of the laws governing the formation of the vapour phase. That is the reason why a lot of the attempts to reveal systematic trends in transition of components of the condensed phase into the vapour may be found in a number of surveys.[1, 2, 8, 9, 111] Knowledge of a variety of species that may form in the vapour as a result of dissociation, association, and polymerization processes is important also from the practical point of view since incongruent selective vapourization of the condensed phase components may deteriorate the performance of high-temperature materials. It should be underlined that all the $Cs_2O$-, SrO-, and BaO-containing systems in most cases will obey the regularities revealed in the high-temperature behaviour of the oxide systems mentioned.

In reviews and monographs,[1, 2, 8, 9, 111] the progress in the studies of the vapourization processes in the oxide systems over the last 10 years was analyzed. The general acid-base concept of vapourization of oxide systems was developed.[1, 2, 8, 9, 111] There were also the description of the advantages and reliability of HTMS method providing the unique thermodynamic information that is crucial for predicting and modelling of physicochemical properties of oxide materials, and outlines possible approaches to classification of types and trends in the formation of the vapour phase composition.

One of the fundamental points of the analysis is the acid-base concept used in the study[8, 111] considering the electron potentials (or electronegativities) of oxides defined as the ratio of the first ionization energy of the element forming the oxide to the radius of the ion of this element in the corresponding oxidation state. As an example, the available data on ternary silicate systems composed of different number of glass-formers and glass-modifiers are discussed.

Based on the previous data on the binary systems a conclusion was made that the vapour composition strongly depends on the number of outer valence electrons of the oxide-modifier. The degree of association increases with atomic number of oxide-modifiers in the lower rows of the Periodic Table. This fact may be connected with the participation of d- and f-electrons in the chemical bonds. The following parameters must be taken into account to understand the vapourization behaviour of the binary oxide systems from the point of view of the acid-base concept such as

— values of the differences of electron potentials of the elements forming oxides;

— enthalpies of formation of oxide-modifier;

— the lattice energy of oxide-modifier per mole of $O^{2-}$ at the temperature 298 K;

— the energies of the $M-O-X$ bond (M is the element of the glass modifier, X = B, Si).

Analysis of dependences of these parameters on the mass number of the element of the oxide-modifier indicates that one of the main reasons for the decrease in the polymerization level from 3 to 2 observed in the alkali borates with increasing atomic mass of elements is the decrease in the lattice energy of oxide-modifier per mole of $O^{2-}$ at 298 K and the increase in the enthalpy of formation of oxide modifier. Correlation of the values of the maximum differences of electron potentials of the elements forming oxides in binary systems, from which multicomponent melts can be composed, with the information on the relative concentration of gaseous monomers of borates and their dimers in the vapour over them, makes it possible to estimate the tendency to association and polymerization of oxides in the vapour over multicomponent systems.

Additional criteria that should be taken into consideration when comparing the volatility of oxide systems include

— the ratio of the partial pressures of molecular forms in the vapour over individual oxides measured at the same temperature;

— the tendency to association of these molecular forms for pairs of oxides forming a multicomponent system;

— the relative content of oxides in the condensed phase of a multicomponent system;

— the values of oxygen partial pressures characterizing the acid-base properties of oxide melts.[8, 111]

The following guidelines are relevant for predicting the relative volatility of the binary and multicomponent oxide systems, *e.g.*,

— in a series of melts with a common oxide-modifier an increase of volatility of components in the order from silicate to borate melts is observed, as a consequence of growing acidity of the melts in the indicated order;

— the most abundant species in the vapour over the silicate glass-forming melts are the forms characteristic of dissociative vapourization of the oxides forming the systems;

— in the vapour over borate melts containing oxides of alkali metals, beryllium, lead, bismuth or barium, the formation of gaseous borates is most probable and their polymerized forms may exist;

— in multicomponent alkaline boron-silicate melts with the content of boron oxide higher than that of alkali metals oxides and silica, alkaline borates were the main vapour species.[8, 111]

The data listed in Table 14 illustrating the vapourization features of ternary systems containing among others cesium, strontium, and barium oxides confirms the validity of the proposed criteria. The vapour species over systems Nos $8-13$ are the same as over individual oxides, whereas the vapourization in systems Nos $1-7$ proceeds with the formation of gaseous salts and dimers in addition to $B_2O_3$ and SiO present in the vapour over individual oxides.

Thus, the latest results obtained by HTMS confirm that it remains one of the most informative and powerful methods in the high-temperature thermodynamic studies. Its reliability is commonly proved by mutual consistency of the results and their reasonable agreement with the results obtained by alternative more precise methods, such as high temperature calorimetry. Another evidence of the high

**Table 14**. Composition of the vapour over ternary silicate systems studied by the KEMS approach.[111]

| No | System under study | Vapourization temperature, K | Identified vapour species |
|----|--------------------|-----------------------------|----------------------------|
| 1 | $Na_2O - B_2O_3 - SiO_2$ | 1200 | $NaBO_2$, $(NaBO_2)_2$, $B_2O_3$ |
| 2 | $Cs_2O - B_2O_3 - SiO_2$ | 1020 | $CsBO_2$, $(CsBO_2)_2$, $B_2O_3$ |
| 3 | $Rb_2O - B_2O_3 - SiO_2$ | 900 | $RbBO_2$, $(RbBO_2)_2$, $B_2O_3$ |
| 4 | $MgO - B_2O_3 - SiO_2$ | 1550 − 1800 | $MgBO_2$, $MgB_2O_4$, $B_2O_3$, $SiO$, $O_2$ |
| 5 | $CaO - B_2O_3 - SiO_2$ | 1800 | $CaBO_2$, $CaB_2O_4$, $B_2O_3$, $SiO$, $O_2$ |
| 6 | $SrO - B_2O_3 - SiO_2$ | 1720 | $SrBO_2$, $SrB_2O_4$, $B_2O_3$, $SiO$, $O_2$ |
| 7 | $BaO - B_2O_3 - SiO_2$ | 1650 | $BaBO_2$, $BaB_2O_4$, $B_2O_3$, $SiO$, $O_2$ |
| 8 | $PbO - B_2O_3 - SiO_2$ | 1100 | $PbO$, $Pb$, $O_2$ |
| 9 | $ZnO - B_2O_3 - SiO_2$ | 1100 | $Zn$, $O_2$ |
| 10 | $MgO - Al_2O_3 - SiO_2$ | 1770 − 1940 | $Mg$, $SiO$, $O_2$ |
| 11 | $CaO - Al_2O_3 - SiO_2$ | 1800 − 2000 | $Ca$, $CaO$, $CaSiO_3$, $AlSiO$, $Al$, $AlO$, $SiO$, $O_2$ |
| 12 | $CaO - TiO_2 - SiO_2$ | 1800 − 2000 | $Ca$, $CaO$, $TiO_2$, $TiO$, $SiO$, $O_2$ |
| 13 | $BaO - TiO_2 - SiO_2$ | 1800 − 2000 | $Ba$, $BaO$, $TiO_2$, $TiO$, $SiO$, $O_2$ |

quality of the data provided by HTMS is their conformity with the information of phase diagrams of the systems studied. The correlation of thermodynamic properties of a system obtained by high temperature mass spectrometry with the information on the phase diagrams was observed for example in the case of the $CaO - SiO_2$, $MgO - SiO_2$, and $MgO - Al_2O_3 - SiO_2$ systems.[8]

In addition, the advantages of the HTMS method as source of the experimental data used for high-temperature thermodynamic modelling within the GLTAS approach are rendered in Refs 111, 112, 113. Development of this theory for the calculation of thermodynamic properties was carried out for the ternary silicate melts with one oxide-modifier and one glass-forming oxide in the $CaO - Al_2O_3 - SiO_2$, $CaO - TiO_2 - SiO_2$ and $BaO - TiO_2 - SiO_2$ systems and with one oxide-modifier and two glass-forming oxides in the $Na_2O - B_2O_3 - SiO_2$ and $Cs_2O - B_2O_3 - SiO_2$ systems. In some cases, the lattice chosen for the optimization of the experimental data may be considered as a model of the real melt structure and then the optimized energy parameters may be identified with the energies of chemical bonds in the melt. The validity of such interpretation in a particular case of the $SrO - B_2O_3 - SiO_2$-melts structure was confirmed by the direct experimental studies of glasses in this system by the X-ray scattering method.[83]

It should be underlined that the data on thermodynamic properties of the Cs-, Sr-, and Ba-containing oxide systems at high temperatures summarized in the present review may be valuable input for the further development of the modern thermodynamic data bases used for modelling and prediction of the phase diagram of multicomponent systems such as NUCLEA[114–116] or TAF-ID[117] data bases.

The results of recent of studies of the vapourization processes in the Cs-, Sr-, and Ba-bearing oxide systems valuable for analysis of severe accidents in nuclear power plants are summarized in the review. The key role of the Knudsen effusion mass spectrometric method in obtaining the data on the gas phase composition over these systems, their thermodynamic properties, and relative volatility of components in different series of oxide systems is demon-

strated. It is shown that the main features of vapourization of the Cs-, Sr-, and Ba-bearing oxide systems are as follows:

— transition of the molecular forms into vapour may be accompanied by the reactions of dissociation, association, dimerization;

— the partial pressures of vapour species over oxide systems and materials are measurable by HTMS at the temperatures characteristic of the nuclear reactor core melts and even lower;

— formation of the associated molecular forms (gaseous oxy-acid salts) is typical for many groups of oxide systems and in some cases may prove to be the main mechanism of dispersion of radioactive nuclides in nuclear accidents;

— composition of the vapour phase can be predicted within the acid-base approach using the data on the volatility of the constituent individual oxides;

— the concept of the mean orbital electronegativity is a well-proven quantitative measure of the acidic (basic) properties of oxides;

— correlation between the standard enthalpies of atomization of the oxides can be used for correction of the calculated thermodynamic functions and for their prediction;

— application of more elaborate HTMS techniques may be used for further refinement of the experimental results;

— the data obtained by the Knudsen effusion mass spectrometric method is most advisable as a basis for modelling the thermodynamic properties of melts and glasses by the semi-quantitative and statistical thermodynamics methods.

All these features reflect also the general approaches developed and accepted at present for the predicting and modelling of high temperature behaviour and thermodynamic properties of multicomponent oxide systems. However, the limited information on high temperature behaviour of the Cs-, Sr- and Ba-bearing oxide systems summarized in the present review indicates the necessity for further high temperature mass spectrometric studies of the binary and multicomponent systems containing $Cs_2O$, SrO and BaO required for the solution of the nuclear safety problems. Enlargement of experimental data on the high-temperature vapourization processes and thermodynamic properties of various yet unexplored binary and multicomponent systems containing $Cs_2O$, SrO and BaO will allow to improve the reliability of modern thermodynamic data bases required for the development of the safe technologies and materials for the nuclear industry.

# 8. List of abbreviations and symbols

Abbreviations and symbols used in the text:
EMF — Electromotive force,
Gen IV — Fourth Generation,
GLTAS — Generalized Lattice Theory of Associated Solutions,
HTMS — High Temperature Mass Spectrometry,
KEMS — Knudsen Effusion Mass Spectrometry,
NPP — Nuclear Power Plant,

V.L.Stolyarova, A.L.Shilov, T.V.Sokolova, M.Kurata, D.Costa
*Russ. Chem. Rev.*, 2023, **92** (5) RCR5059

21 of 22

NUCLEA — Thermodynamic database for nuclear applications,

OECD NEA — Organization of Economic Cooperation and Development of Nuclear Energy Agency,

TCOFF — Thermodynamic Characterization Of Fuel debris and Fission products based on scenario analysis of severe accident progression at the Fukushima Daiichi Nuclear Power Station,

$a_i$ — activity of $i$-component

$p_i$ — partial pressure of $i$-vapour species

$\Delta G$ — Gibbs energy of formation,

$\Delta G^{\,E}$ — excess Gibbs energy of formation,

$\Delta H_r$ — enthalpy of reaction,

$\Delta H_s$ — enthalpy of sublimation,

$\Delta H_f$ — enthalpy of formation,

$\Delta H_{at}$ — enthalpy of atomization,

$K_p$ — equilibrium constant of reaction,

$\Delta_r S$ — entropy of reaction,

$\Delta \mu_i$ — chemical potential of $i$-component.

# 9. References

1. V.L.Stolyarova. *Russ. Chem. Rev.*, **85**, 60 (2016)
2. V.L.Stolyarova. *CALPHAD*, **64**, 258 (2019)
3. Yu.A.Zolotov. *J. Tech. Nat. Sci.*, **11**, 117 (2015)
4. R.S.Borisov, O.I.Klychnikov, A.T.Lebedev, V.B.Pronin, A.A.SysoevaV.G.Zaikin. *J. Anal.*, **10**, 1567 (2021)
5. A.I.Rusanov. *Russ. Chem. Rev.*, **85**, 1 (2016)
6. Yu.A.Borisov, A.V.Gusarov, L.N.Gorokhov. *High Temperature*, **2**, 487 (1964)
7. A.V.Gusarov, L.N.Gorokhov. *High Temperature*, **4**, 636 (1966)
8. V.L.Stolyarova, G.A.Semenov. *Mass Spectrometric Study of the Vaporization of Oxide Systems.* (Chichester: Wiley and Sons, 1994). 434 p.
9. E.K.Kazenas. *Termodinamika Ispareniya Dvoinykh Oksidov. (Thermodynamics of Vaporization of Binary Oxides).* (Moscow: Nauka). 551 p.
10. V.L.Stolyarova, A.L.Shilov, O.N.Pestova, T.V.Sokolova. *Nuclear Propulsion Reactor Plants. Life Cycle Management Technologies*, **3**, 37 (2022)
11. T.Kindap, U.Turuncoglu, S.H.Chen, A.Unal, M.Karaca. *Water, Air and Soil Pollution*, **198**, 393 (2009)
12. B.K.Sovacool. *J. Contemporary Asia*, **40**, 369 (2010)
13. A.Yu.Petrov. *Rosenergoatom*, **2**, 4 (2020)
14. V.G.Asmolov. *Sci. Am.*, **2**, 32 (2015)
15. V.S.Arutyunov, G.V.Lisichkin. *Russ. Chem. Rev.*, **86**, 777 (2017)
16. E.Buglova, T.McKenna, V.Kutkov. *Radioprotection*, **48**, S73 (2013)
17. T.McKenna, W.P.Vilar, J.Callen, R.Martincic, B.Dodd, V.Kutkov. *Health Phisics Society*, **108**, 15 (2015)
18. V.Kutkov, V.V.Tkachenko, S.P.Saakian. *Nuclear Energy and Technology*, **2**, 24 (2016)
19. V.Kutkov, V.V.Tkachenko. *Nuclear Energy and Technology*, **3**, 38 (2017)
20. A.P.Moller, T.A.Mousseau. *Trends Ecol. Evol.*, **21**, 200 (2006)
21. M.I.Balonov. *Radiatsiya i Risk*, **15**, 97 (2006)
22. Y.Shibahara, T.Kubota, T.Fujiia, S.Fukutani, T.Ohta, K.Takamiya, R.Okumura, S.Mizuno, H.Yamana. *J. Nucl. Sci. Technol.*, **51**, 575 (2014)
23. S.Bechta, W.Ma, A.Miassoedov, C.Journeau, K.Okamoto, D.Manara, D.Bottomley, M.Kurata, B.R.Sehgal, J.Stuckert, M.Steinbrueck, B.Fluhrer, T.Keim, M.Fischer, G.Langrock, P.Piluso, Z.Hozer, M.Kiselova, F.Belloni, M.Schyns. *Ann. Nucl. Energy*, **124**, 541 (2019)
24. S.I.Lopatin, S.M.Shugurov, V.L.Stolyarova, N.G.Tyurnina. *Russ. J. Gen. Chem.*, **76**, 1878 (2006)
25. V.L.Stolyarova, S.I.Lopatin, N.G.Tyurnina. *Dokl. Phys. Chem.*, **411**, 309 (2006)
26. V.L.Stolyarova, S.I.Lopatin, S.M.Shugurov, N.G.Tyurnina. *Dokl. Phys. Chem.*, **411**, 315 (2006)
27. Patent RU 2192053 C1 (2002)
28. Patent RU 2212719 C2 (2003)
29. Patent FI 118445 (2007)
30. V.V.Gusarov, V.I.Almjashev, V.B.Khabensky, S.V.Bechta,V.S.Granovsky. *Zh. Ros. Khim. Ob-va im. D.I.Mendeleeva*, **49**, 42 (2005)
31. Patent RU 2586224 C1 (2016)
32. V.B.Khabensky, V.S.Granovsky, A.A.Sulaczkij, M.B.Sulaczkaya, V.I.Almjashev. *Atom. Ehnerg.*, **132**, 116 (2022)
33. M.I.Ojovan, P.P.Poluektov. *Priroda*, **3**, 3 (2010)
34. M.Ojovan, P.Poluektov, V. Kascheev. *Nucl. Eng. Int.*, **7**, 28 (2012)
35. V.I.Almjashev, V.B.Khabensky, V.S.Granovsky, E.V.Krushinov, S.A.Vitol, A.A.Sulatsky, E.V.Shevchenko. *Atom. Enegr.*, **132**, 110 (2022)
36. M.I.Ojovan, W.E.Lee. *New Developments in Glassy Nuclear Wasteforms.* (Nova Sci. Publ., 2007). 135 p.
37. Patent RU 2176830 C2 (2001)
38. Y.Shibahara, T.Kubota, T.Fujii, S.Fukutani, T.Ohta, K.Takamiya, R.Okumura, S.Mizuno, H.Yamana. *J. Nucl. Sci. Technol.*, **51**, 575, (2014)
39. P.Singh, M.Bandyopadhyay, K.Pandya, M.Bhuyan, A.Chakraborty. *Nucl. Fusion*, **59**, 106023 (2019)
40. Patent RU 2569651 C1 (2015)
41. M.H.Langowski, J.G.Darab, P.A.Smith. *PNNL-11052 UC-512 Project Technical Information* (1996)
42. S.Bechta, W.Ma, A.Miassoedov, C.Journeau, K.Okamoto, D.Manara, D.Bottomley, M.Kurata, B.R.Sehgal, J.Stuckert, M.Steinbrueck, B.Fluhrer, T.Keim, M.Fischer, G.Langrock, P.Piluso, Z.Hozer, M.Kiselova, F.Belloni, M.Schyns. *Ann. Nucl. Energy*, **124**, 541 (2019)
43. G.Balducci, A.Ciccioli, G.De.Maria, F.Hodaj, G.M.Rosenblatt. *Pure Appl. Chem.*, **81**, 299 (2009)
44. J.Drowart, C Chatillon, J.Hastie, D.Bonnell. *Pure Appl. Chem.*, **77**, 683 (2005)
45. A.S.Smirnov, N.A.Gribchenkova, A.S.Alikhanyan. *J. Chem. Technol.*, **22**, 427 (2021)
46. F.-Z.Roki, C.Chatillon, M.-N.Ohnet, D.Jacquemain. *J. Chem. Thermodynam.*, **40**, 401 (2008)
47. F.-Z.Roki, M.-N.Ohnet, S.Fillet, C.Chatillon, I.Nuta. *J. Chem. Thermodynam.*, **65**, 247 (2013)
48. F.-Z.Roki, M.-N.Ohnet, S.Fillet, C.Chatillon, I.Nuta. *J. Chem. Thermodynam.*, **70**, 46 (2014)
49. K.Nakajima, T.Takai, T.Furukawa, M.Osaka. *J. Nucl. Mater.*, **491**, 183 (2017)
50. V.L.Stolyarova, S.I.Lopatin, G.A.Sycheva, E.N.Plotnikov. *Glass Phys. Chem.*, **31**, 789 (2005)
51. V.L.Stolyarova, V.A.Vorozhtcov, S.I.Lopatin, S.M.Shugurov, E.P.Simonenko, N.P.Simonenko, M.Kurata, D.Costa. *Rapid Commun. Mass Spectrom.*, **35**, e9079 (2021)
52. E.H.P.Cordfunke, R.J.M.Konings, E.F.Westrum. *Thermochim. Acta*, **128**, 31 (1988)
53. R.Vandeputte, D.Khiri, C.Lafont, L.Cantrel, F.Louis. *J. Nucl. Mater.*, **517**, 63 (2019)
54. E.L.Kozhina, M.M.Shultz. *Glass Phys. Chem.*, **22**, 477 (1996)
55. V.L.Stolyarova, S.I.Lopatin, O.L.Belousova, L.V.Grishchenko. *Glass Phys. Chem.*, **32**, 55 (2006)
56. E.N.Plotnikov, V.L.Stolyarova. *Glass Phys. Chem.*, **32**, 181 (2006)
57. V.L.Stolyarova, S.I.Lopatin, E.N.Plotnikov. *Glass Phys. Chem.*, **32**, 543 (2006)
58. E.N.Plotnikov, V.L.Stolyarova. *Glass Phys. Chem.*, **32**, 550 (2006)
59. V.L.Stolyarova. *J. Non-Cryst. Solids*, **354**, 1373 (2008)
60. R.Odoj, K.Hilpert. *Z. Naturforsch.*, **35a**, 9 (1980)
61. E.K.Kazenas, I.O.Samoylova, G.K.Astakhova. *Russ. Metallurgy (Metally)*, **4**, 38 (1997)

22 of 22

V.L.Stolyarova, A.L.Shilov, T.V.Sokolova, M.Kurata, D.Costa
*Russ. Chem. Rev.*, 2023, **92** (5) RCR5059

62. V.L.Stolyarova, V.A.Vorozhtcov, S.I.Lopatin, S.M.Shugurov, E.P.Simonenko, N.P.Simonenko, M.Kurata, D.Costa. *Rapid Commun. Mass Spectrom.*, **35**, e9097 (2021)

63. I.Johnson. *J. Phys. Chem.*, **79**, 722 (1975)

64. M.Yamawaki, T.Oka, M.Yasumoto, H.Sakurai. *J. Nucl. Mater.*, **201**, 257 (1993)

65. E.K.Kazenas, I.O.Samoilova, G.K.Astakhova. *Russ. Met.*, **4**, 39 (1997)

66. S.I.Lopatin, G.A.Semenov, T.S.Pilyugina. *Zh. Obshch. Khim.*, **70**, 529 (2000)

67. E.K.Kazenas, I.O.Samoylova, G.K.Astakhova, A.A.Petrov. *Russian Metallurgy (Metally)*, **6**, 14 (2001)

68. S.I.Lopatin, G.A.Semenov, T.S.Pilyugina. *Russ. J. Gen. Chem.*, **72** (12), 1857 (2002)

69. S.I.Lopatin, S.M.Shugurov, V.L.Stolyarova, N.G.Tyurnina. *Russ. J. Gen. Chem.*, **76**, 1878 (2006)

70. T.Kou, M.Asano. *High Temp. Sci.*, **24**, 1 (1987)

71. M.Asano, T.Kou. *J. Chem. Thermodynam.*, **20** (10), 1149 (1988)

72. M.Asano, T.Kou. *J. Chem. Thermodynam.*, **22**, 1223 (1990)

73. T.Kou, M.Asano. *Bull. Inst. Atom. Energy Kyoto Univ.*, **73**, 49 (1988)

74. T.Kou, M.Asano. *Bull. Inst. Atom. Energy Kyoto Univ.*, **73**, 50 (1988)

75. M.Asano, T.Kou. *High Temp. Sci.*, **29**, 171 (1990)

76. M.Asano, T.Kou. *Bull. Inst. Atom. Energy Kyoto Univ.*, **74**, 56 (1988)

77. M.Asano, T.Kou. *Bull. Inst. Atom. Energy Kyoto Univ.*, **74**, 57 (1988)

78. M.Asano, T.Kou. *J. Chem. Thermodynam.*, **21**, 837 (1989)

79. S.I.Lopatin, G.A.Semenov, V.I.Baranovskii, S.M.Shugurov, V.V.Sizov. *Russ. J. Gen. Chem.*, **71**, 1342 (2001)

80. S.I.Lopatin, V.L.Stolyarova, N.G.Tyurnina, Z.G.Tyurnina. *Russ. J. Gen. Chem.*, **76**, 1687 (2006)

81. V.L.Stolyarova, S.I.Lopatin, N.G.Tyurnina. *Dokl. Phys. Chem.*, **411**, 309 (2006)

82. V.L.Stolyarova, S.I.Lopatin, S.M.Shugurov, N.G.Tyurnina. *Dokl. Phys. Chem.*, **411**, 315 (2006)

83. V.L.Stolyarova, S.I.Lopatin, A.L.Shilov. *Russ. J. Gen. Chem.*, **79**, 1778 (2009)

84. S.I.Lopatin, G.A.Semenov, S.M.Shugurov. *Russ. J. Gen. Chem.*, **73**, 169 (2003)

85. E.K.Kazenas, Yu.V.Tsvetkov, I.O.Samoilova, G.K.Astakhova, V.A.Volchenkova. *Russ. Metallurgy (Metally)*, **2008**, 104 (2008)

86. E.K.Kazenas, Yu.V.Tsvetkov, G.K.Astakhova, I.O.Samoilova, V.A.Volchenkova. *Russ. Metallurgy (Metally)*, **2007**, 105 (2007)

87. S.I.Lopatin, G.A.Semenov. *Rus. J. Gen. Chem.*, **71**, 1522 (2001)

88. E.Rangel-Salinas, A.Pisch, C.Chatillon, C.Bernard. *ECS Transactions*, **3**, 87 (2007)

89. G.A.Semenov, S.I.Lopatin. *Rus. J. Gen. Chem.*, **71**, 828 (2001)

90. S.M.Shugurov, S.I.Lopatin. *J. Chem. Thermodynam.*, **37**, 715 (2005)

91. S.M.Shugurov, S.I.Lopatin. *Russ. J. Gen. Chem.*, **76**, 871 (2006)

92. V.L.Stolyarova, S.I.Lopatin, A.A.Selyutin, V.A.Vorozhtcov, S.M.Shugurov. *Russ. J. Inorg. Chem.* **67**, 2077 (2022)

93. V.L.Stolyarova, V.A.Vorozhtsov, S.I.Lopatin, A.A.Selyutin, S.M.Shugurov, A.L.Shilov, V.A.Stolyarov, V.I.Almjashev. *Rapid Commun. Mass Spectrom.*, **37**, e9459 (2023)

94. D.-H.Peck, M.Miller, K.Hilpert. *J. Electrochem. Soc.*, **148**, A657 (2001)

95. I.Yu.Archakov, V.L.Stolyarova, M.M.Shultz. In *V Ural skaya Konferentsiya po Fizicheskoi Khimii i Elektrokhimii Ionnykh Rasplavov i Tverdykh Elektrolitov. (Vth Ural Conference on Physical Chemistry and Electrochemistry of Ionic Melts and Solid Electrolytes)*. (Sverdlovsk: UO Akad. Nauk SSSR, 1989). P. 11

96. V.L.Stolyarova, I.Yu.Archakov, M.M.Shultz. In *Proceedings of the Sundaram Symposium, An International Symposium on Thermochemistry and Chemical Processing*. (Ed. C.K.Mathews). (Kalpakkam, India: The Indian Institute of Metals, 1991). P. 429

97. E.H.P.Cordfunke, R.J.M.Konings, R.R.Laan, W.Ouweltjes. *J. Chem. Thermodynam.*, **25**, 343 (1993)

98. S.I.Lopatin, G.A.Semenov, S.M.Shugurov. *Russ. J. Gen. Chem.*, **71**, 61 (2001)

99. E.H.P.Cordfunke, C.P.Groen, M.E.Huntelaar, C.A.Alexander, J.S.Ogden. *J. Chem. Thermodynam.*, **32**, 839 (2000)

100. S.I.Lopatin, S.M.Shugurov, V.L.Stolyarova, Z.G.Tyurnina. *J. Chem. Thermodynam.*, **38**, 1706 (2006)

101. V.L.Stolyarova, S.I.Lopatin, S.M.Shugurov, Z.G.Tyurnina. *Dokl. Phys. Chem.*, **407**, 85 (2006)

102. Z.G.Tyurnina, V.L.Stolyarova, S.I.Lopatin, E.N.Plotnikov. *Dokl. Phys. Chem.*, **409**, 186 (2006)

103. Z.G.Tyurnina, S.I.Lopatin, V.L.Stolyarova. *Rus. J. Gen. Chem.*, **78**, 14 (2008)

104. S.I.Lopatin, S.M.Shugurov, G.A.Semenov. *Russ. J. Gen. Chem.*, **73**, 1866 (2003)

105. E.K.Kazenas, Yu.V.Tsvetkov, I.O.Samoilova, G.K.Astahova, A.A.Petrov. *Russ. Metallurgy (Metally)*, **1**, 14 (2003)

106. E.K.Kazenas, Yu.V.Tsvetkov, I.O.Samoilova, G.K.Astahova, A.A.Petrov, B.A.Volchenkova. *Russ. Metallurgy (Metally)*, **4**, 34 (2003)

107. S.I.Lopatin, S.M.Shugurov, G.A.Semenov. *Dokl. Phys. Chem.*, **386**, 255 (2002)

108. V.L.Stolyarova, S.I.Lopatin, S.M.Shugurov. *Dokl. Phys. Chem.*, **397**, 158 (2004)

109. S.I.Lopatin, S.M.Shugurov, A.I.Panin. *Rapid Commun. Mass Spectrom.*, **30**, 2027 (2016)

110. J.W.Hastie. *Pure Appl. Chem.*, **56**, 1583 (1984)

111. V.L.Stolyarova. *ECS Transactions*, **46**, 55 (2013)

112. V.L.Stolyarova, S.I.Lopatin. *Vestn. KGTU*, **1**, 98 (2010)

113. A.L.Shilov, V.L.Stolyarova. *Rus. J. Gen. Chem.*, 80, 2414 (2010)

114. V.A.Vorozhtcov, D.A.Yurchenko, V.I.Almjashev, V.L.Stolyarova. *GlassPhys. Chem.*, **47**, 417 (2021)

115. NUCLEA: Thermodynamic Database for Nuclear Applications [Electronic resource]; http://thermodata.online.fr/nuclea.html (access date 05.05.2023)

116. S.Bakardjieva, M.Barrachin, S.Bechta, P.Bottomley, L.Brissoneau, B.Cheynet, E.Fischer, C.Journeau, M.Kiselova, L.Mezentseva. *Prog. Nucl. Energy*, **52**, 84 (2010)

117. https://www.oecd-nea.org/jcms/pl_24703/thermodynamics-of-advanced-fuels-international-database-taf-id (access date 05.05.2023)